SIAM J. APPL. MATH.
Vol. 78, No. 2, pp. 651–676

TOWARDS A STATIONARY MONGE–KANTOROVICH DYNAMICS: THE PHYSARUM POLYCEPHALUM EXPERIENCE*

ENRICO FACCA†, FRANCO CARDIN†, AND MARIO PUTTI†

Abstract. In this work we propose an extension to the continuous setting of a model describing the dynamics of slime mold, Physarum Polycephalum (PP), which was proposed to simulate the ability of PP to find the shortest path connecting two food sources in a maze. The original model describes the dynamics of the slime mold on a finite-dimensional planar graph using a pipe-flow analogy whereby mass transfer occurs because of pressure differences with a conductivity coefficient that varies with the flow intensity. This model has been shown to be equivalent to a problem of "optimal transportation" on graphs. We propose an extension that abandons the graph structure and moves to a continuous domain. The new model couples an elliptic diffusion equation enforcing PP density balance with an ordinary differential equation governing the flow dynamics. We conjecture that the new system of equations presents a time-asymptotic equilibrium and that such an equilibrium point is precisely the solution of Monge–Kantorovich partial differential equations governing optimal transportation problems. To support this conjecture, we analyze the proposed model by recasting it into an infinite-dimensional dynamical system. We are then able to show well-posedness of the proposed model for sufficiently small times under the hypotheses of Hölder continuous diffusion coefficients and essentially bounded forcing functions. Numerical results obtained with a simple fixed-point iteration combining $\mathcal{P}_1/\mathcal{P}_0$ finite elements with backward Euler time stepping show that the approximate solution of our formulation of the transportation problem converges at large times to an equilibrium configuration that well compares with the numerical solution of the Monge–Kantorovich equations.

Key words. slime-mold dynamics, Monge–Kantorovich transport problem, dynamic formulation, numerical solution

AMS subject classifications. 49K20, 49M25, 35J70, 65N30

DOI. 10.1137/16M1098383

1. Introduction.

In a recent paper, [19] proposed a mathematical model governing the dynamics of a unicellular slime mold named *Physarum Polycephalum* (PP) that, on the basis of experimental evidence [18], grows following the most efficient network path between food sources. The experiments suggest that the PP slime, after colonization of the entire maze paths, evolves along the shortest path connecting the two food sources. PP abilities have been used for the experimental analysis of transportation networks, with many researchers suggesting that this slime mold is capable of identifying the optimal many-site connecting transportation network, with applications to such systems as the railroads of Tokyo and Spain [20, 1]. Many further surprising properties of PP have been experimentally identified, but in this work we are interested in studying and extending the mathematical model proposed by [19] to describe the slime-mold dynamics.

The original model of [19] reads as follows. Given a undirected planar graph $G = (E, V)$ with positive edge length $\{L_e\}_{e\in E}$, find the edge function D_e and the

*Received by the editors October 11, 2016; accepted for publication (in revised form) October 2, 2017; published electronically March 1, 2018.
http://www.siam.org/journals/siap/78-2/M109838.html
†Department of Mathematics "Tullio Levi-Civita", University of Padua, via Trieste 63, Padova, 35121 Italy (facca@math.unipd.it, cardin@math.unipd.it, putti@math.unipd.it).

vertex function p_v that satisfy

$$\sum_{e\in\sigma(v)} Q_e(t) = f_v \quad \text{(balance law-Kirchoff)} \qquad \forall v \in V, \tag{1.1a}$$

$$Q_e(t) = D_e(t)\frac{(p_u(t) - p_v(t))}{L_e} \quad \text{(Fick–Poiseuille)} \qquad \forall e = (u, v) \in E, \tag{1.1b}$$

$$D_e'(t) = g\left(|Q_e(t)|\right) - D_e(t) \quad (D_e \text{ dynamics}) \qquad \forall e = (u, v) \in E, \tag{1.1c}$$

$$D_e(0) = \hat{D}_e(0) > 0 \quad \text{(initial data)} \qquad \forall e = (u, v) \in E, \tag{1.1d}$$

where $e = (u, v)$ denotes the edge of G connecting vertices u and v, the vertex source function f_v satisfies the compatibility condition of an isolated system $\sum_{v\in V} f_v = 0$ [6, 7], where $\sigma(v)$ is the "star" of v, i.e., the set of edges having vertex v in common, and $g : \mathbb{R}^+ \mapsto \mathbb{R}^+$ is a nondecreasing function with $g(0) = 0$. This model can be explained heuristically using a classical hydraulic analogy, eventually motivating the above introduced terms "balance law-Kirchoff" and "Fick–Poiseuille." We think of the graph G as representing the set of pipes where the flow of a fluid driven by the vertex source function f_v occurs. Then, (1.1a) can be identified as the enforcement of the fluid mass balance, while (1.1b) is the momentum balance stating that the flux in each graph edge is proportional to the discrete gradient of the vertex potential function p_v via a conductance coefficient D_e (inverse of a resistance). Hydraulic resistance to flow is known to be proportional to the pipe perimeter, and hence to its diameter. Thus, the evolutive equation (1.1c), which forms the innovative core of the model, asserts the intuitive behavior that to optimally (with minimal energy loss) accommodate larger fluxes the pipe diameter must increase, although it needs to remain bounded. From this observation it can be concluded that the function $g(x)$ must be nondecreasing. Moreover, to avoid unboundedness, the growth of the hydraulic conductivity needs to be compensated for by introducing the balancing decay term $-D_e(t)$. In [19] several numerical results using this model were presented. The most relevant to our study are those where the vertex source function was concentrated in the first (1) and last (n) vertex of the graph (the entrance and exit of the fluid in the hydraulic analogy), i.e., $f_1 = -f_n = 1$ and $f_v = 0$ for $1 < v < n$. Using this setting, numerical evidence shows that when $g(x) = x$ the conductivity D_e at large times tends to localize (have a nonzero support) on the edges of the shortest path between the two external sources. This has been confirmed more recently by [6, 7], who show that indeed, for $t \to \infty$, the distribution of D_e converges to the shortest path. Moreover, the same authors prove that the above model is equivalent to an optimal transport (OT) problem on the graph G and can be recast as the problem of finding $Q = \{Q_e\}_{e\in E}$ such that

$$\begin{aligned} &\min_{Q\in\{Q_e\}_{e\in E}} J(Q), \qquad J(Q) := \sum_{e\in E} Q_e L_e, \\ &\text{s.t.:} \\ &\sum_{e\in\sigma(v)} Q_e = f_v \qquad \text{for all } v \in V. \end{aligned}$$

In fact, under some general assumptions on the graph structure, the solution of system (1.1) converges to a stationary solution $\bar{Q}$ that also solves the above OT problem in G.

In this work we generalize the model given in (1.1) by removing the graph structure and defining the problem on an open bounded domain $\Omega \subset \mathbb{R}^n$. We restrict this study to the case of $g(x) = x$. Then, given a source function $f : \Omega \to \mathbb{R}$, a continuous

analogue of (1.1) tries to find the pair of functions $(\mu, u) : [0, +\infty[\times\Omega \mapsto \mathbb{R}^+ \times \mathbb{R}^n$ that satisfies

$$-\nabla\cdot\Big(\mu(t,x)\nabla u(t,x)\Big) = f(x) \qquad \left(\int_\Omega f\,dx = 0\right), \tag{1.2a}$$

$$\mu'(t,x) = \mu(t,x)\Big(|\nabla u(t,x)| - 1\Big), \tag{1.2b}$$

$$\mu(0,x) = \mu_0(x) > 0, \tag{1.2c}$$

complemented by zero Neumann boundary conditions. Here, μ' indicates partial differentiation with respect to time, and $\nabla = \nabla_x$. This generalization is intuitively justified by comparing the different components of models (1.1) and (1.2). In fact, (1.2a) states the spatial balance of a (continuum) Fick–Poiseuille flux $q = -\mu\nabla u$ with potential function u, while (1.2b) introduces the dynamics postulated in the original discrete model. To address the dynamics of PP in the maze, we need to reconcile the model with the fact that some portions of the domain (the maze barriers in this case) may hinder throughflow. This can be obtained by forcing the gradient to be large where the flux must be small, thus forcing the conductivity μ to become small via the action of the elliptic partial differential equation (PDE) (1.2a). This is obtained by replacing (1.2b) with

$$\mu'(t,x) = \mu(t,x)\Big(|\nabla u(t,x)| - k(x)\Big), \tag{1.3}$$

where $k(x)$ is a positive function describing the spatial pattern of the resistance to flow, whereby large values of k imply large gradients of the potential u and thus large energy losses. In fact, the elliptic equation forces larger gradients to correspond to smaller conductivities and hence smaller fluxes. Note that the partial theoretical results that follow are not influenced by the presence of a sufficiently regular $k(x)$, and we restrict this study to the case $k(x) = 1$. On the other hand, the numerical tests fully consider a spatially variable $k(x)$, showing that the model is not restricted to the uniform case.

In the present paper, we analyze from an analytical and numerical point of view the continuous model of slime-mold dynamics described above, and we conjecture that, like its discrete counterpart, its solution tends to an equilibrium point as time goes to infinity and that this equilibrium point satisfies (the) Monge–Kantorovich (MK) OT problem [14]. We first study existence and uniqueness of the solution of (1.2) for the case $k \equiv 1$, corresponding to the original MK problem. The more general case with heterogeneous $k(x)$ is a straightforward adaptation, at least for smooth enough k. For $k \equiv 1$, if an equilibrium point exists for $t \to +\infty$, then $\mu' \to 0$. Hence, (1.2b) becomes a constraint imposing that, for μ strictly greater than or equal to zero, the norm of the gradient of u must be unitary. This observation is crucial to the development of our conjecture, which reads as follows.

CONJECTURE 1.1. *The solution of* (1.2) *tends as* $t \to \infty$ *to the solution of the following problem: find* $(\mu^*, u^*) \in (L^\infty(\Omega), Lip_1(\Omega))$ *with* $Lip_1(\Omega)$ *the space of Lipschitz continuous functions with unit constant, such that*

$$\begin{aligned} &-\nabla\cdot(\mu^*(x)\nabla u^*(x)) = f^+(x) - f^-(x) = f(x) && \text{in } \Omega,\\ &|\nabla u^*(x)| \le 1 && \text{in } \Omega,\\ &|\nabla u^*(x)| = 1, && \text{where } \mu^*(x) > 0. \end{aligned} \tag{1.4}$$

These equations constitute the PDE-based formulation of the classical optimal transport problem and are named the MK equations [8, 14, 2]. In the past few years they have been the subject of a number of studies that have shed light into regularity and integrability properties of the *OT density* μ^* in relation to the regularity and integrability of the forcing function f [13], and its uniqueness [15].

In this work we show the applicability of the proposed model to the simulation of the dynamics of PP, but, most notably, we try to point out some theoretical and numerical evidence in support of the above conjecture. From the theoretical point of view, we first prove the local-in-time existence and uniqueness of the solution pair (μ, u) in Hölder spaces. To this aim, we recast the problem in operatorial form and look for the functions $u(t)$ and $\mu(t)$ such that

$$\int_\Omega \mu(t)\nabla u(t)\nabla\varphi\, dx = \int_\Omega f\varphi\, dx \qquad \forall\varphi \in H^1(\Omega), \tag{1.5a}$$

$$\mu'(t) = \mathcal{Q}\left(\mu(t)\right) - \mu(t), \qquad \mu(0) = \mu_0, \tag{1.5b}$$

where $\mathcal{Q}(\mu)$ is the operator associated with the weak form (1.5a) of the elliptic PDE (1.2a) that maps μ into $\mu|\nabla u|$. To simplify notation, we consider the dependence on $x \in \Omega$ implicit in all the relevant functions. For a given $\mu > 0$, we denote by $\mathcal{U}(\mu)$ the unique weak solution of the elliptic PDE associated with μ. Clearly, the solution $\mu(t)$ remains bounded as long as the left-hand side remains negative, i.e., $|\nabla\mathcal{U}(\mu(t))| \leq 1$. Standard regularity theory of elliptic PDEs ensures that, for any source function $f \in L^\infty(\Omega)$, the operator $\mathcal{Q}(\mu)$ is well-defined (meaning problem (1.2a) is well-posed, i.e., the associated bilinear form is coercive and continuous) for $\mu(t, x)$, Hölder continuous, and strictly greater than zero. We are then able to show that the operator $\mathcal{Q}(\mu)$ is locally Lipschitz continuous, and we can then invoke Banach–Caccioppoli fixed-point theorems to show local existence and uniqueness of the solution pair (μ, u). However, the fact that Lipschitz continuity is only local in μ, which is a consequence of the need to maintain coercivity of the diffusion equation (1.2a), prevents the extension of this result to larger times. Nevertheless we are able to identify a Lyapunov-candidate function $\mathcal{L}$, i.e., a function whose time derivative along the flow trajectories (its Lie derivative) is nonpositive.

Next, on the basis of these findings, we experiment numerically on the large time behavior of the proposed system (1.2) together with the extended dynamics (1.3). Given a triangulation of the domain Ω, the discrete model uses a $\mathcal{P}_1$ Galerkin approach for the discretization of the potential u and a $\mathcal{P}_0$ Galerkin scheme for the discretization of the diffusion coefficient μ. To avoid oscillations on the numerical gradient, we use different approximation spaces for u and μ by defining the $\mathcal{P}_1$ potential on a uniformly refined mesh, an approach reminiscent of the inf-sup stable $\mathcal{P}_1$-iso-$\mathcal{P}_2/\mathcal{P}_1$ Stokes finite element method (FEM) spaces. This methodology leads to a coupled differential algebraic system of equations that is solved by a simple forward Euler method. The resulting numerical algorithm is applied for the solution of the dynamics of PP on the maze.

The conjecture that problems (1.2) and (1.4) are asymptotically equivalent finds application to the numerical solution of the OT equations as, from preliminary experimental evidence, convergence to an asymptotic state seems smooth and fast even using the low order standard $\mathcal{P}_1/\mathcal{P}_0$ Galerkin approximations described above and on relatively coarse meshes. The conjecture is supported experimentally by comparing our numerical solution against the numerical results presented in [4], where the solution to (1.4) was obtained by means of RT0 mixed finite elements and automatic

mesh refinement on a larger triangulation and with much higher computational costs. Eventually, from a numerical point of view, the above asymptotic behavior seems rather robust under successive mesh refinements.

2. Main results. In this section we lay down the technical results about our slime-mold dynamics gained in a rather sharp and convenient functional environment. The main idea consists of the synthesis of the proposed dynamics towards an infinite-dimensional abstract ODE that passes through a standard elliptic setting. We obtain a theorem about local existence and uniqueness, but at present we are not able to extend this result to larger times. Nevertheless, an interesting Lyapunov-candidate function $\mathcal{L}$ is inherited by invoking the analogy of our problem at infinite time with the PDE based OT setting and its relationship with the shape optimization problem. Assuming existence of the solution and its first time derivative at all times, we prove that $\mathcal{L}$ is always decreasing in time and reaches stationarity at $t = \infty$. Although we are not currently able to use it properly, this result seems promising in the search for a global existence theorem and a formal justification of the conjecture that the proposed slime-mold problem is, at infinite time, equivalent to the MK problem.

2.1. Notations. We will denote by $\mathcal{F}$ the set of essentially bounded functions f with zero mean and compact support in an open, bounded, convex, and simply connected subset Ω of $\mathbb{R}^n$:

$$\mathcal{F} := \left\{ f \in L^\infty(\Omega) : \operatorname{supp}(f) \subsetneq \Omega \text{ and } \int_\Omega f\, dx = 0 \right\}.$$

Without loss of generality, we may redefine the domain of f by means of an n-dimensional ball $B(0, \bar{R})$ with $\bar{R}$ sufficiently large so that $\Omega \subset B(0, \bar{R})$ and with $f = 0$ outside of Ω (in most cases of interest Ω can be an n-dimensional interval). We will still use the same symbol Ω to denote such a subset. We define the subset $\mathcal{D}$ of $\mathcal{C}^\delta(\bar{\Omega})$ as

$$\mathcal{D} := \left\{ \mu \in \mathcal{C}^\delta(\bar{\Omega}) : \lambda(\mu) := \min_{x \in \bar{\Omega}} \mu(x) \geq \alpha > 0 \right\},$$

where

$$\mathcal{C}^\delta(\bar{\Omega}) = \left\{ v : \bar{\Omega} \mapsto \mathbb{R} \ : \ v_{[\delta,\bar{\Omega}]} := \sup_{x \neq y} \frac{|v(x) - v(y)|}{|x - y|^\delta} < +\infty \right\},$$
$$\|v\|_{\mathcal{C}^\delta(\bar{\Omega})} := \sup_{\bar{\Omega}} v + v_{[\delta,\bar{\Omega}]}$$

with $\delta \in]0, 1[$. We indicate with $\mathcal{C}^{1,\delta}(\bar{\Omega})$ the Hölder space of continuously differentiable functions with first derivatives in $\mathcal{C}^\delta(\bar{\Omega})$. In the proof of Theorem 2.6, we will be using the following characterization of the subspace $\mathcal{D}$. Given $0 < a < b < \infty$, the subspace $\mathcal{D}$ can be redefined as the union of open and convex subsets:

$$\mathcal{D} = \bigcup_{0<a<b<+\infty} \mathcal{D}(a, b); \quad \mathcal{D}(a, b) := \left\{ \mu \in \mathcal{C}^\delta(\bar{\Omega}) a < \lambda(\mu) \leq \|\mu\|_{\mathcal{C}^\delta(\bar{\Omega})} < b \right\}. \tag{2.1}$$

Standard results on regularity theory of elliptic PDEs [16] allow us to give the following definitions.

DEFINITION 2.1 (potential). *Let $\mu \in \mathcal{D}$ and $f \in \mathcal{F}$. The operator $\mathcal{U} : \mathcal{D} \mapsto \mathcal{C}^{1,\delta}(\bar{\Omega})$ maps μ into $\mathcal{U}(\mu)$, where $\mathcal{U}(\mu)$ is the unique weak solution of the elliptic equation* (1.2a)*, i.e.,*

$$\int_\Omega \mu \nabla u \cdot \nabla \varphi \, dx = \int_\Omega f\varphi \, dx \quad \forall \varphi \in H^1(\Omega), \qquad s.t. \int_\Omega u \, dx = 0.$$

Remark 2.2. Note that the vanishing of the average of u ensures the uniqueness of $\mathcal{U}$.

DEFINITION 2.3 (flux). *Let $\mu \in \mathcal{D}$ and $f \in \mathcal{F}$. The operator $\mathcal{Q} : \mathcal{D} \mapsto \mathcal{C}^{\delta}(\bar{\Omega})$ is defined as $\mu \mapsto \mathcal{Q}(\mu) := \mu|\nabla \mathcal{U}(\mu)|$.*

2.2. Local existence and a Lyapunov-candidate function. In this section we report the main results and developments that lead to the local well-posedness of the model and to the identification of the proposed Lyapunov-candidate function. We start by writing the weak formulation of system (1.2) for a zero-mean function $u(t, x)$:

$$\int_\Omega \mu(t,x)\nabla u(t,x)\nabla\varphi(x)\, dx = \int_\Omega f(x)\varphi(x)\, dx \quad \forall \varphi \in H^1(\Omega), \tag{2.2a}$$

$$\mu'(t,x) = \mu(t,x)|\nabla u(t,x)| - \mu(t,x), \tag{2.2b}$$

$$\mu(0,x) = \mu_0(x) \in \mathcal{D}. \tag{2.2c}$$

Definitions 2.1 and 2.3 allow us to substitute the potential $\mathcal{U}(\mu)$ into (2.2b) to obtain the following semilinear evolution equation

$$\mu'(t) = -\mu(t) + \mathcal{Q}(\mu(t)), \qquad \mu(0) = \mu_0 \in \mathcal{D}, \tag{2.3}$$

where the dependence on x has been omitted. Obviously, the pair $(\mu(t,x), u(t,x))$ can be reconstructed from $(\mu(t), \mathcal{U}(\mu(t)))$. The mild formulation of (2.3) is given by

$$\mu(t) = e^{-t}\mu_0 + \int_0^t e^{s-t}\mathcal{Q}\left(\mu(s)\right) ds. \tag{2.4}$$

The Banach–Caccioppoli fixed-point theory states that local existence and uniqueness of (2.3) require that the operator $\mathcal{Q}(\mu)$ be locally Lipschitz continuous. We have the following propostion.

PROPOSITION 2.4. *The potential and flux operators $\mathcal{U}$ and $\mathcal{Q}$ are Lipschitz continuous and bounded in $\mathcal{D}(a,b)$ for all a and b, $0 < a < b < \infty$.*

In other words we have that for every $\mu \in \mathcal{D}(a,b)$,

$$\|\mathcal{U}(\mu)\|_{\mathcal{C}^{1,\delta}(\bar{\Omega})} \le C_1(a,b) \quad \text{and} \quad \|\mathcal{Q}(\mu)\|_{\mathcal{C}^{\delta}(\bar{\Omega})} \le C_2(a,b)$$

and there exist constants $L_{\mathcal{U}}(a,b)$ and $L_{\mathcal{Q}}(a,b)$ such that, for every $\mu_1, \mu_2 \in \mathcal{D}(a,b)$,

$$\|\mathcal{U}(\mu_1) - \mathcal{U}(\mu_2)\|_{\mathcal{C}^{1,\delta}(\bar{\Omega})} \le L_{\mathcal{U}}(a,b)\|\mu_1 - \mu_2\|_{\mathcal{C}^{\delta}(\bar{\Omega})},$$
$$\|\mathcal{Q}(\mu_1) - \mathcal{Q}(\mu_2)\|_{\mathcal{C}^{\delta}(\bar{\Omega})} \le L_{\mathcal{Q}}(a,b)\|\mu_1 - \mu_2\|_{\mathcal{C}^{\delta}(\bar{\Omega})}.$$

The previous proposition follows from the next lemma.

LEMMA 2.5. *Let $\mu \in \mathcal{D}$, $F_0 \in \mathcal{F}$, and $F = (F_i)_{(i=1,\dots,n)} \in [\mathcal{C}^\delta(\bar\Omega)]^n$ and $u \in H^1(\Omega)$ be the unique solution of*

$$\int_\Omega \mu \nabla u \cdot \nabla \varphi \, dx = \int_\Omega (F_0 \varphi + F \cdot \nabla \varphi) \, dx \quad \forall \varphi \in H^1(\Omega) \quad s.t. \quad \int_\Omega u \, dx = 0.$$

Then $u \in \mathcal{C}^{1,\delta}(\bar\Omega)$ and the following estimate holds:

$$\|\nabla u\|_{\mathcal{C}^\delta(\bar\Omega)} \le K_\delta(n,\Omega,\delta) K_\mu(\mu) \left(\|F_0\|_{L^\infty(\Omega)} + \|F\|_{\mathcal{C}^\delta(\bar\Omega)} \right), \tag{2.5}$$

where $K_\delta(n,\Omega,\delta)$ is a constant depending on the dimension n, the domain Ω, and the Hölder regularity δ of μ, and

$$K_\mu(\mu) = K_\mu\left(\lambda(\mu), \|\mu\|_{\mathcal{C}^\delta(\bar\Omega)}\right) = \frac{1}{\lambda(\mu)} \left(\frac{\|\mu\|_{\mathcal{C}^\delta(\bar\Omega)}}{\lambda(\mu)} \right)^{\frac{n+\delta}{2\delta}}. \tag{2.6}$$

This lemma, whose proof is given in subsection 4.6, extends classical results of regularity theory of elliptic equations with Hölder continuous coefficients by careful estimation of the dependence upon $\mu \in \mathcal{D}$ of the constants K_δ and K_μ [21, 16]. The latter result allows us to prove the main theorem of the paper:

THEOREM 2.6. *Given $\mu_0 \in \mathcal{D}$ there exists $\tau(\mu_0) > 0$ such that the Cauchy problem (2.3) admits a unique solution $\mu \in \mathcal{C}^1\left([0,\tau(\mu_0)[; \mathcal{C}^\delta(\bar\Omega)\right)$. Moreover, this solution remains strictly greater than zero and*

$$\lambda(\mu(t)) \ge e^{-t} \lambda(\mu_0) \tag{2.7}$$

for $t \in [0,\tau(\mu_0)[$.

This theorem suggests that there must be an interplay between μ and $\nabla\mathcal{U}$ that constrains the flux $|\mathcal{Q}|$ to remain bounded so that, under the hypotheses of Theorem 2.6, existence and uniqueness of the solution pair (μ, u) are expected for all times. However, such a global result seems out of reach within the current framework because the conclusions of Lemma 2.5 do not allow us to improve the local Lipschitziness of $\mathcal{U}$ and $\mathcal{Q}$. Nonetheless, local existence and uniqueness of the solution, albeit incomplete, offer a certain degree of confidence on the correctness of the model of the PP dynamics, and justify the use of numerical discretizations to supply credible evidence that the model is well-posed for all times.

A further indication that the problem is globally well-posed is provided by the fact that we have identified a Lyapunov-candidate function $\mathcal{L}$, i.e, a function with a nonpositive Lie derivative. The derivation borrows from results in the field of mass/shape optimization by considering its relationship with OT problems and starts by defining the shape optimization problem as described in [8].

Assume we have two nonnegative functions f^+ and f^- in Ω, with $\int_\Omega f^+ = \int_\Omega f^-$, representing, e.g., the density of a given electric charge, and a fixed amount of a conductive material, described by a nonnegative function σ having unit mass. Interpreting Ω as an insulating medium, we ask the question of how to optimally distribute the given conductive material so that the heating induced by the current flow from f^+ to f^- is minimal. In [8] the authors consider the case where f^+, f^-, and σ are nonnegative Radon measures and discuss the connection between the mass optimization problem and a generalized version of the MK equations. They proved that the optimal distribution of conductive material σ^* given f^+ and f^- is the normalized optimal transport density μ^* of the MK equations with $f = f^+ - f^-$. Thus the two

problems are equivalent up to a multiplicative constant. In the case of $f \in \mathcal{F}$, these results together with those given in [13] lead to the following formulation:

$$\min_{\sigma\in\mathcal{M}} \mathcal{E}(\sigma) = \frac{1}{2}\int_\Omega \sigma|\nabla\mathcal{U}(\sigma)|^2, \qquad \mathcal{M} = \left\{\sigma \in L^\infty(\Omega) \ : \int_\Omega \sigma\, dx = 1\right\}.$$

Recasting the shape optimization intuition into the framework of our formulation, it is natural to identify a density $\sigma(t) = \left(\mu(t)/\int_\Omega \mu(t)\, dx\right)$ that belongs to $\mathcal{M}$. Then, following our conjecture that $\mu(t) \to \mu^*$ as $t \to \infty$, it is natural to assume that $\sigma(t)$ should tend to σ^*, the solution of the shape optimization problem. Noting that $\mathcal{U}(\sigma) = \left(\int_\Omega \mu\, dx\right)\mathcal{U}(\mu)$, we can define $\mathcal{L}$ as

$$\mathcal{L}(\mu) := \frac{1}{2}\int_\Omega \mu\, dx \cdot \int_\Omega \mu|\nabla\mathcal{U}(\mu)|^2\, dx. \tag{2.8}$$

Intuitively, we are looking for a density μ that gives the best trade-off between the total mass, and thus the cost of the transport infrastructure and the dissipated energy. For increasing time, the above function $\mathcal{L}$ evaluated along the trajectory $\mu(t)$ decreases towards a stationary condition, as the following theorem states.

THEOREM 2.7. *The function $\mathcal{L} : \mathcal{D} \longmapsto \mathbb{R}^+$ defined above is strictly decreasing in time along the solution $\mu(t)$ for $t \in [0, \tau(\mu_0)[$.*

The previous theorem leads to the following lemma.

LEMMA 2.8. *For all $t \in [0, \tau(\mu_0)[$ the L^1-norm of $\mu(t)$ and $\mathcal{Q}(\mu(t))$ are bounded by constants depending only on the initial data μ_0.*

3. Numerical solution. In this section we describe the numerical discretization used to find an approximate solution to the proposed model, and report the numerical results obtained solving the proposed model to simulate the PP dynamics on the maze. Next we report some numerical results aimed at justifying the conjecture that the solution of the proposed time-dependent model tends as time tends to infinity to the solution of the MK problem. To this aim, the model is applied to the solution of the OT problems proposed by [4] and the numerical results are compared.

3.1. Spatial and temporal discretization. The numerical solution of (2.2) is obtained by means of the method of lines. We denote with $\mathcal{T}_h(\Omega)$ and $\mathcal{T}_{2h}(\Omega)$ two regular triangulations of the domain Ω, where $\mathcal{T}_h$ is obtained from $\mathcal{T}_{2h}$ by connecting the edge midpoints. Indicating by N_{2h}, E_{2h}, and M_{2h} the number of nodes, edges, and triangles of mesh $\mathcal{T}_{2h}$, respectively, we have that $N_h = N_{2h} + E_{2h}$ and $M_h = 4M_{2h}$. Spatial discretization is achieved using standard Galerkin finite elements by projecting (2.2a) onto the finite-dimensional space $V_h(\Omega) = \mathcal{P}_1(\mathcal{T}_h(\Omega)) = \text{span}\{\varphi_1(x), \ldots, \varphi_{N_h}(x)\}$ of piecewise linear Lagrangian basis functions defined on $\mathcal{T}_h(\Omega)$ and (2.2b) onto the finite-dimensional space $W_h(\Omega) = \mathcal{P}_0(\mathcal{T}_{2h}(\Omega))$ of piecewise constant functions. Following this approach, let $u_h(t,x) \in L^2([0,T]; V_h(\Omega))$ be the spatially discrete potential and $\mu_h(t,x) \in L^2([0,T]; W_h(\Omega))$ the diffusion coefficient. We obtain the following system of differential algebraic equations.

Find $(u_h, \mu_h) \in V_h \times W_h$ such that $\int_\Omega u_h \, dx = 0$ and

$$a_{\mu_h}(u_h, \varphi_m) = \int_\Omega \mu_h \nabla u_h \cdot \nabla \varphi_m \, dx = \int_\Omega f \varphi_m \, dx, \qquad m = 1, \dots, N_h, \tag{3.1a}$$

$$\int_\Omega \mu_h' \chi_s \, dx = \int_\Omega \mu_h \left(|\nabla u_h| - k \right) \chi_s \, dx, \qquad s = 1, \dots, M_{2h}, \tag{3.1b}$$

$$\int_\Omega \mu_h(0, \cdot) \chi_s \, dx = \int_\Omega \mu_0 \chi_s \, dx, \qquad s = 1, \dots, M_{2h}. \tag{3.1c}$$

Forward Euler time stepping discretizes (3.1b) yielding a decoupled system of linear equations. Denoting with Δt_j the time-step size so that $t_{j+1} = t_j + \Delta t_j$ and writing $u_h^j \approx u_h(t_j, x)$ and $\mu_h^j \approx \mu_h(t_j, x)$, the final solution algorithm can be written as

$$a_{\mu_h^j}(u_h^j, \varphi_m) = (f, \varphi_m), \qquad m = 1, \dots, N_h, \tag{3.2a}$$

$$\mu_s^{j+1} = \mu_s^j \left(1 + \Delta t_j (|\nabla u_h^j|_s - k_s) \right), \qquad s = 1, \dots, M_{2h}, \tag{3.2b}$$

where

$$a_{\mu_h^j}(u_h^j, \varphi_m) = \int_\Omega \mu_h^j \nabla u_h^j \cdot \nabla \varphi_m \, dx = \sum_{l=1}^{N_h} u_l^j \int_\Omega \mu_h^j \nabla \varphi_l \cdot \nabla \varphi_m \, dx,$$

and $|\nabla u_h|_s$, k_s, and μ_s^0 indicate the integral averages over triangle T_s. Equation (3.2a) is a sparse system of linear equations of dimension N_h, and is solved by means of the incomplete Choleski preconditioned conjugate gradient with the variant proposed by [5] to solve the corresponding semidefinite linear system arising in our pure Neumann problem. The $M_{2h} \times M_{2h}$ linear system described in (3.1b) is diagonal and leads to (3.2b). To maintain the coercivity of the FEM bilinear form $a_{\mu_h^j}(\cdot, \cdot)$ we impose a lower bound on μ_h of 10^{-10}.

Remark 3.1. The choice of the two different FEM spaces V_h and W_h, which resemble the inf-sup stable $\mathcal{P}_1$-iso-$\mathcal{P}_2/\mathcal{P}_1$ FEM spaces for the Stokes equation [9], is dictated by the need to reduce or eliminate oscillations on the gradient $|\nabla u_h|$ that occur if different approximating spaces are used. Experimentally, in fact, we observed that in the case $(u_h, \mu_h) \in \mathcal{P}_1(\mathcal{T}_h) \times \mathcal{P}_0(\mathcal{T}_h)$, oscillations in ∇u_h appear and destroy convergence of the numerical solution. On the other hand, using the proposed approach $(u_h, \mu_h) \in \mathcal{P}_1(\mathcal{T}_h) \times \mathcal{P}_0(\mathcal{T}_{2h})$, which essentially is nothing else than a simple average of the solution gradient on the larger triangles, all the oscillations disappear.

3.2. Numerical simulation of PP dynamics. The proposed model and its numerical discretization just described are applied to the simulation of the dynamics of the experiment described in [19, 18]. The domain encompassing the entire maze setup is discretized by means of a uniform triangulation obtained by subdividing each edge of the square-shaped maze into 128 subdivisions yielding the coarser mesh $\mathcal{T}_{2h}$ comprised of 32768 elements and 16641 nodes. This high resolution is required to follow accurately the walls of the maze, which are described by setting $k(x) = 1000$ (brown colors in the upper left panel of Figure 1) while the maze paths are characterized by $k(x) = 1$. These values are calibrated experimentally to enforce that flux through the maze walls is practically impeded. The initial condition μ_0 is set to 10^{-10} on the maze walls and one elsewhere. The two food sources $f^+ = 1$ and $f^- = -1$ are shown as red squares in Figure 1. We employ a variable time-step size

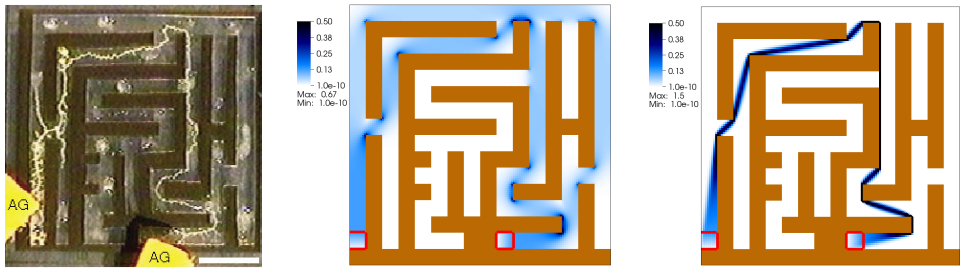

FIG. 1. *Simulation of the dynamics of PP mass reorganization in the maze experiment of* [19, 18]*: distribution of PP transport density at dimensionless times* $t = 60.3$ *(central panel), and* $t = 9.6 \times 10^3$ *(right panel), compared to the experimental distribution shown on the left (from* [18]*, reprinted with permission). The simulation was done on a triangulation* $\mathcal{T}_{2h}$ *with* 32768 *triangles and* 16641 *nodes. At the last time step of the simulation, the* μ_h *variation was smaller than* $\tau = 5 \times 10^{-9}$.

starting from $\Delta t_0 = 10^{-2}$ and with $\Delta t_{j+1} = \min(1.01\Delta t_j, 0.5)$ to ensure stability of the forward Euler scheme is verified for all times with an ample safety margin. The simulation is stopped when the relative difference in μ_h becomes smaller than the tolerance τ, i.e.,

$$\text{var}(\mu_h(t^j)) = \frac{\|\mu_h^{j+1} - \mu_h^j\|_{L^2(\Omega)}}{\Delta t_j \|\mu_h^j\|_{L^2(\Omega)}} \leq \tau \tag{3.3}$$

with $\tau = 5 \times 10^{-9}$. Figure 1 shows the distribution of μ_h at two different times, chosen in agreement with the simulations reported in [19, 18]. These times are useful to identify the intermediate phase when the PP starts retreating from the dead ends ($t = 60.3$) and the final steady-state configuration achieved at $t = 9.6 \times 10^3$. Note that the same numerical solution is obtained, albeit at different dimensionless times, starting from different initial conditions μ_0. The central panel of Figure 1 shows the intermediate phase when PP completely retreated from the dead end paths of the maze but persists on all the possible paths connecting the two food sources. We note a stronger concentration of μ_h at the edges of the maze walls, indicating that PP starts accumulating around a narrow band along the shortest route. At the final time (right panel), μ_h is distributed along the optimal route displaying varying approximation levels depending on the alignment of the mesh triangles with the support of μ_h. In fact, the vertical portion is one element thick, while the oblique routes encompass more than one triangle. This is a common feature that is reproduced experimentally at all mesh refinement levels. All these observations are in line with the results proposed by [19], although in our case the graph structure is not imposed a priori but it is mimicked through the appropriate definition of $k(x)$. Note that in our continuous setting the presence of $k(x)$ is related to the cost of throughflow, while the original graph-based formulation allows only flow through the graph edges.

3.3. Numerical simulation of OT problems. In this section we report numerical evidence supporting the conjecture that the long-time solution of the slime-mold dynamic model is a solution of the MK equations (1.4). To this aim we compare our solution with the one proposed by [4]. At the same time, the aim of this section is to show that the solution of the MK equations by means of the proposed dynamic model is numerically easier than the direct solution of system (1.4), suggesting that the introduction of time relaxes the numerical difficulties yielding a more robust, flexible, and efficient method for the numerical solution of OT problems.

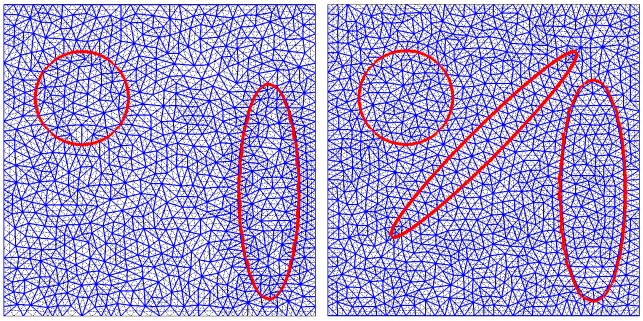

FIG. 2. *Unit square domain and triangulations $\mathcal{T}_{2h}$ (solid blue) and $\mathcal{T}_h$ (dotted black) for the homogeneous (left) and heterogeneous (right) test cases. The supports of f^+ (left circle) and f^- (right ellipse) are shown in red, as well as the central ellipse where $k(x)$ is different from the background in the heterogeneous case.*

We apply the numerical approach described above to the solution of the homogeneous and heterogeneous model problems proposed in Example 1 of [4]. These problems consider a unit square domain with zero Neumann boundary and constant forcing having uniform positive value (f^+) supported on a circle and uniform negative value (f^-) on an ellipse in such a way that spatial balance is ensured (Figure 2). The domain contains a central oblique oval shape where a value for $k(x)$ different from the unitary background value is specified. Four different test cases are defined. The first one, called the homogeneous test case, considers a unit value of $k(x)$ assigned in the entire domain. This corresponds to the standard MK equation reported in system (1.4). Then three heterogeneous problems are addressed by setting the value of $k(x)$ in the central oblique ellipse equal to $k_e = 0.01$ and $k_e = 100$, respectively. The former case favors flow through the central oval, while the latter impedes it. The final test case considers an intermediate value of $k_e = 3$ in the central oval and is used to show the dynamical behavior of the proposed model by looking at the numerical solution at intermediate times.

To accurately impose the forcings of the different problems, the triangulations are adapted to the supports of $f(x)$ and $k(x)$, compelling the use of nonuniform meshes. The homogeneous case is solved on a sequence of three uniformly refined triangulation pairs $\mathcal{T}_{2h}(\mathcal{T}_h)$. The coarsest mesh has 820(3170) nodes and 1531(6124) triangles (Figure 2, left), for a total of $4701 (= 3170 + 1531)$ degrees of freedom in the final algebraic solution algorithm (3.2). The next two levels have 3170(12463) and 6124(24496) triangles, yielding a total of 18587 degrees of freedom, and 12463(49421) nodes and 24496(97984) triangles, for a total of 73917 degrees of freedom, respectively. In the heterogeneous case we employ two triangulation levels starting with a mesh of 933(3603) nodes and 1738(6952) elements (Figure 2, right). All simulations start with a spatially uniform unitary initial condition μ_h^0 and are run until condition (3.3) is satisfied with $\tau = 5 \times 10^{-9}$. The sequence of time-step sizes is the same as in the case of the slime mold simulation, but with different upper bounds to ensure stability of the Euler scheme at large times.

The experimental results for the homogeneous test case are shown in Figure 3, where the spatial distributions of μ_h^j and $|\nabla u_h^j|$ are plotted for the coarser ($\mathcal{T}_h$) mesh at the three refinement levels. All the features of the expected solution of the MK problem are present in these results, which are in good agreement with those of [4]. The support of the transport density concentrates on the region connecting the circle

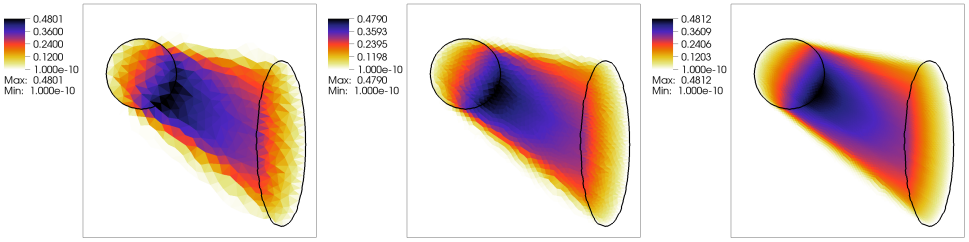

FIG. 3. *Numerical solution of the homogeneous OT problem: distribution of the transport density μ_h at three different mesh refinement levels of the coarser ($\mathcal{T}_{2h}$) triangulation (from left to right).*

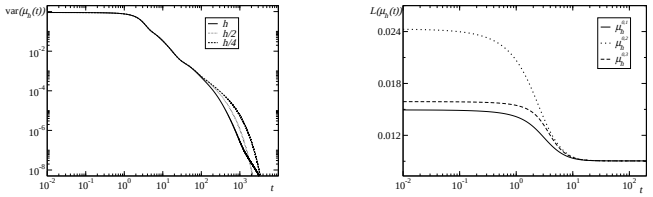

FIG. 4. *Numerical results for the homogeneous OT problem. Left panel: convergence towards zero of the relative variation of the transport density* $\mathrm{var}(\mu_h(t^j)) = \|\mu_h^{j+1} - \mu_h^j\|_{L^2(\Omega)} / (\Delta t_j \|\mu_h^j\|_{L^2(\Omega)})$ *for the three refinement levels. Right panel: behavior of* $\mathcal{L}(\mu_h(t^j))$ *versus time for the three different initial data* ($\mu^0_{h,1}$, $\mu^0_{h,2}$, $\mu^0_{h,3}$) *and the coarsest mesh level.*

boundaries with the ellipse. Along the transport rays, μ_h increases from zero to its maximum value within the supports of f^+ and then decreases moving towards the ellipse, tending to negligible values at ray ends [14, 10]. The norm of the gradient, not shown for brevity, is practically one in all triangles of $\mathcal{T}_{2h}$ lying within the support of μ_h. All these features are clearly visible already at the coarsest level, although the effects of large elements is evident. At increasing mesh refinements the delineation of the support of μ_h is sharper, and at the final level the accuracy seems to be satisfactory and compares well with the solution proposed by [4].

Convergence toward steady state is monotonic, as shown in Figure 4 (left), where the relative variation of $\mathrm{var}(\mu_h(t))$ is shown in log-log scale as a function of time for the three refinement levels. We notice that the convergence behavior is identical for all refinement levels up to a relative μ_h variation of approximately 10^{-3}, which corresponds to a dimensionless time $\hat{t} \approx 60$. At this point the discretization errors seem to slightly influence convergence. We note that from this time on the value of $\mathcal{L}$ (Figure 4, right panel) is practically constant, suggesting that the solution has effectively converged to a stationary state. At the first refinement level, the number of time steps to reach $\hat{t}$ is 431, while 6641 is the number of time steps at the final time $t^* = 3200$ (the upper bound on Δt_j is 0.25). The average number of iterations of the IC0-preconditioned conjugate gradient per time step is 66.

The model solution at large times is insensitive to the distribution of μ_h^0 as shown by the behavior of $\mathcal{L}$ reported in the right panel of Figure 4, where three different sets of initial data, $\mu_h^{0,i}$, $i = 1, 2, 3$, are tested:

$$\mu^0_{h,1}(x,y) = 1, \quad \mu^0_{h,2}(x,y) = 0.1 + 4\left((x-0.5)^2 + (y-0.5)^2\right),$$
$$\mu^0_{h,3}(x,y) = 3 + 2\sin(8\pi x)\sin(8\pi y).$$

This result is upheld by the fact that $\mathcal{L}(\mu_h)$ numerically evaluated starting from three

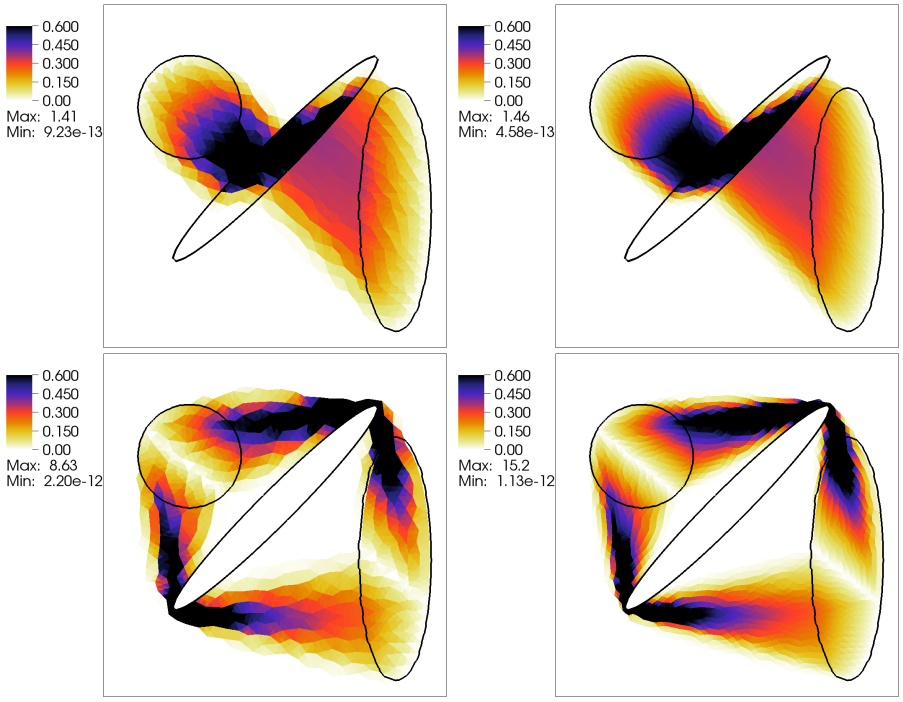

FIG. 5. *Numerical solution of the heterogeneous test case for* $k_e = 0.01$ *(top) and* $k_e = 100$ *(bottom) in the central ellipse. The figures show the OT flux magnitude* $|q_h| = \mu_h|\nabla u_h|$ *for the mesh with* 1738(6952) *triangles and* 933(3603) *(left) and the once-refined mesh* 6952(27808) *triangles and* 3603(14157) *nodes (right).*

different initial conditions always converges to the same value (Figure 4, right). Its nonincreasing behavior shows that $\mathcal{L}$ is a plausible candidate for a Lyapunov function.

In this work we are not interested in implementing the most computational efficient algorithm but we want to show that simple numerical methods are sufficient to find an accurate solution to the MK equations. We would like to remark that many improvements can be done to the numerical scheme and are indeed under development. Notwithstanding its simplicity, our approach is competitive with respect to more direct MK solution methods, such as the one proposed in [4]. These authors solve the direct OT problem using a mixed FEM with adaptive mesh refinement that converged to a final triangular grid adapted to the shape of the transport plan. The discretization on the final mesh level leads to a final nonlinear system with approximately 60000 degrees of freedom which is solved by an ad hoc nonlinear successive overrelaxation method. The successive overrelaxation method used to solve the nonlinear system was considered converged when the relative flux residual was smaller than 10^{-3}. Noting that in this case the convergence criteria based on relative variations of μ_h or on $|q_h| = \mu_h|\nabla u_h|$ are equivalent, as stated above, from Figure 4 we see that this convergence level is reached at $\hat{t} \approx 60$ in our case. At this time, our Lyapunov-candidate function has reached an almost steady condition with a very small rate of decrease, signaling that for practical purposes convergence to the sought solution has been achieved.

The numerical results for the heterogeneous case are shown in Figure 5 where the steady-state spatial distribution of the flux magnitude $|q_h| = \mu_h|\nabla u|$ is plotted in the

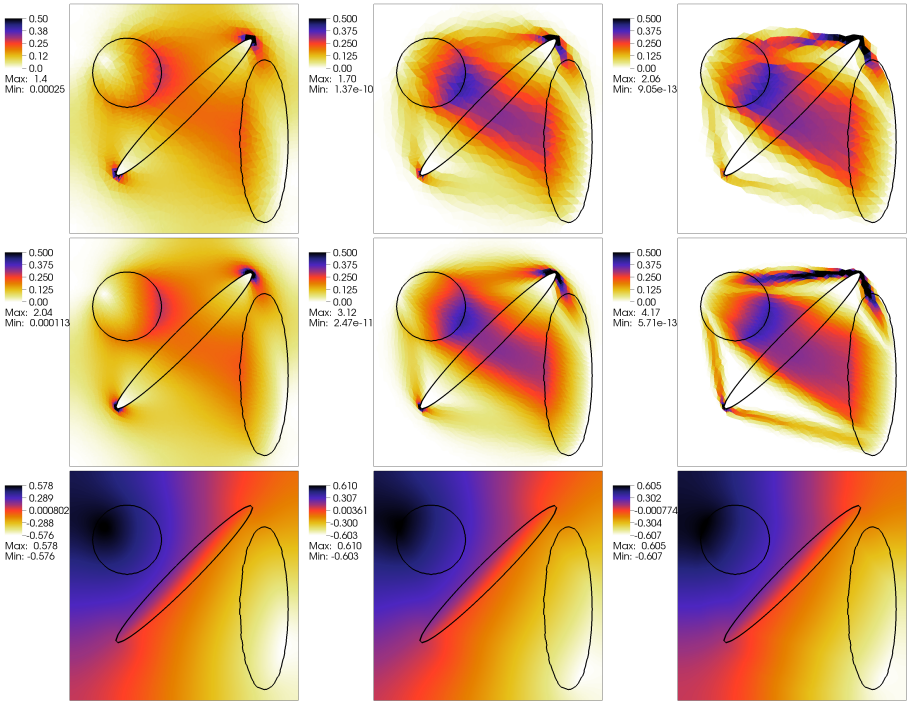

FIG. 6. *Numerical solution of the heterogeneous test case with $k_e = 3$ in the central ellipse in terms of OT flux magnitude $|q_h| = \mu_h|\nabla u_h|$ at the three different times characterized by* $\mathrm{var}(\mu_h) = 0.1, 0.01$, *and* 5×10^{-9} *(left to right) and two refinement levels (upper and central row). The lower row contains the spatial distribution of the potential u_h at the same times for the finest mesh level.*

case of $k_e = 0.01$ (top panels) and $k_e = 100$ (bottom panels). We first note that in this heterogeneous case the gradient is bounded by $k(x)$ and not by one as in the previous test case. For this reason we chose to plot the flux magnitude $|q_h| = \mu_h|\nabla u_h|$ instead of μ_h. Two successively refined triangulations are used, leading to linear systems of dimensions $N_h + M_{2h} = 3603 + 1738$ and $N_h + M_{2h} = 14157 + 6952$ for the coarser and the finer meshes, respectively. The results are comparable with those of [4], although obtained with a much coarser discretization. It is interesting to note that the qualitative features of the solution are obtained already at the coarser mesh, with no visible numerical artifacts barring mesh roughness. We would like to stress here the fact that, notwithstanding the use of a mesh with nodes that are not aligned with the support of μ_h, the geometrical features of the solution are well captured at all mesh resolution levels. From the spatial distribution of the flux magnitude, we see that values of k_e lower than one promote larger fluxes across the central ellipses. On the contrary, values substantially larger than one restrict throughflow, and promote the circumnavigation of the low conductivity areas.

Finally, Figure 6 shows the distribution of $|q_h| = \mu_h|\nabla u_h|$ for the case of $k_e = 3$ at three different times (left to right) and two successive refinement levels (top and central rows), and of the potential u_h (bottom row). The three times are chosen so that the μ_h variation reaches the thresholds $\mathrm{var}(\mu_h(\hat{t}_1)) = 0.1$, $\mathrm{var}(\mu_h(\hat{t}_2)) = 0.01$, and $\mathrm{var}(\mu_h(\hat{t}_3)) = 5 \times 10^{-9}$. Correspondingly, we have $\hat{t}_1 \approx 5.2$ and $\hat{t}_2 \approx 21$, remaining the same for both tested triangulations, and $\hat{t}_3 = 1600$ for the coarser level and $\hat{t}_3 = 2200$ for the finer mesh as steady state is achieved at a later time for the finer

mesh, reflecting the fact that the overall error is smaller. In fact, the converged steady-state solution occurs after 6616 and 8955 time steps for the coarse and fine triangulations, respectively. Note that, for this last heterogeneous test case, the time-stepping sequence employed an upper bound on Δt_j equal to 0.25. Also in this case the steady-state numerical solution is similar to the results reported by [4]. We see from the time sequence that our model constructs the transport map gradually. Starting from the uniformly distributed initial condition, it first identifies the larger flow paths and then refines them to arrive at the final configuration. The spatial distribution of the potential u_h, shown for the same times in the bottom three panels, displays, as expected, a regular behavior typical of elliptic problems. The overall results are consistently pointing towards the veracity of the conjecture that the infinite-time solution to our problem indeed coincides with the solution of the MK equations in the support of the OT path.

4. Proofs of the results.

4.1. Proof of Proposition 2.4: Lipschitz continuity of $\mathcal{U}$ and $\mathcal{Q}$. We start by considering the solution $u \in H^1(\Omega)$ of (1.2a) in weak form:

$$a_\mu(u,\varphi) = \int_\Omega \mu \nabla u \cdot \nabla \varphi \, dx = \int_\Omega f\varphi \, dx \quad \forall \varphi \in H^1(\Omega) \qquad \text{s.t.} \int_\Omega u \, dx = 0, \tag{4.1}$$

where the constraint that u has zero mean ensures uniqueness of the solution. We recall here the general hypotheses for the well-posedness of problem (4.1): (i) the domain Ω is a bounded, connected, and convex subset of $\mathbb{R}^n$ with $\mathcal{C}^1$ or Lipschitz boundary $\partial\Omega$; (ii) $f \in L^2(\Omega)$; (iii) the bilinear form $a_\mu(u,\varphi)$ is bounded and coercive, i.e.,

$$\exists\, 0 < \Lambda < +\infty \quad \text{such that} \quad |a_\mu(u,v)| \le \Lambda \|u\|_{H^1(\Omega)} \|v\|_{H^1(\Omega)} \quad \forall u, v \in H^1(\Omega), \tag{4.2}$$

$$\exists\, 0 < \lambda < +\infty \quad \text{such that} \quad a_\mu(u,u) \ge \lambda \|u\|^2_{H^1(\Omega)} \quad \forall u \in H^1(\Omega). \tag{4.3}$$

It follows from the above that, if $\Omega = B(0,\bar{R})$, $\mu \in \mathcal{D}$, and $f \in \mathcal{F}$, the hypotheses for existence and uniqueness of the elliptic equation are satisfied and thus the operators $\mathcal{U}$ and $\mathcal{Q}$ are well-defined. The regularity result provided in Lemma 2.5 ensures that $\mathcal{U}$ maps into $\mathcal{C}^{1,\delta}(\bar{\Omega})$. Then, given $\mu \in \mathcal{D}(a,b)$ we apply Lemma 2.5 with $F_0 = f$ and $F_i = 0$ to obtain

$$\|\nabla \mathcal{U}(\mu)\|_{\mathcal{C}^\delta(\bar{\Omega})} \le K_\delta(\Omega,n,\delta) K_\mu(a,b) \|f\|_{L^\infty(\Omega)}. \tag{4.4}$$

From this, the boundedness of the potential $\mathcal{U}(\mu)$ follows immediately. The local Lipschitz continuity of $\mathcal{U}$ derives from the following considerations. Given $\mu_1, \mu_2 \in \mathcal{D}(a,b)$ and $u_k = \mathcal{U}(\mu_k)$ with $k = 1,2$, we note that

$$\begin{aligned} \int_\Omega \mu_1 \nabla u_1 \nabla \varphi \, dx &= \int_\Omega f\varphi \, dx = \int_\Omega \mu_2 \nabla u_2 \nabla \varphi \, dx \quad \forall \varphi \in H^1(\Omega), \\ \int_\Omega \mu_1 \nabla (u_1 - u_2) \nabla \varphi \, dx &= \int_\Omega (\mu_2 - \mu_1) \nabla u_2 \nabla \varphi \, dx \quad \forall \varphi \in H^1(\Omega). \end{aligned} \tag{4.5}$$

Application of Lemma 2.5 with $F_0 = 0$ and $F = -(\mu_1 - \mu_2)\nabla \mathcal{U}(\mu_2))$, which belongs to $(\mathcal{C}^\delta(\bar{\Omega}))^n$ because of (4.4), yields

$$\begin{aligned} \|\nabla(u_1 - u_2)\|_{\mathcal{C}^\delta(\bar{\Omega})} &\le K_\delta(\Omega,n,\delta) K_\mu(\mu_1) \|(\mu_1 - \mu_2)\nabla u_2\|_{\mathcal{C}^\delta(\bar{\Omega})} \\ &\le K_\delta(\Omega,n,\delta) K_\mu(\mu_1) \|\mu_1 - \mu_2\|_{\mathcal{C}^\delta(\bar{\Omega})} \|\nabla u_2\|_{\mathcal{C}^\delta(\bar{\Omega})} \\ &= K_\delta(\Omega,n,\delta)^2 K_\mu(a,b)^2 \|f\|_{L^\infty(\Omega)} \|\mu_1 - \mu_2\|_{\mathcal{C}^\delta(\bar{\Omega})}. \end{aligned} \tag{4.6}$$

We can also prove that the flux $\mathcal{Q}$ is bounded in $\mathcal{D}(a,b)$. In fact, since the Hölder norm is submultiplicative, we can write from (4.4),

$$\|\mathcal{Q}(\mu)\|_{\mathcal{C}^\delta(\bar\Omega)} = \|\mu|\nabla\mathcal{U}(\mu)|\,\|_{\mathcal{C}^\delta(\bar\Omega)} \le K_\delta(\Omega,n,\delta)\; b\, K_\mu(a,b)\|f\|_{L^\infty(\Omega)}.$$

Lipschitz continuity of $\mathcal{Q}$ derives from (4.6) as follows:

$$\begin{aligned}\|\mathcal{Q}(\mu_1)-\mathcal{Q}(\mu_2)\|_{\mathcal{C}^\delta(\bar\Omega)} &= \|\mu_1|\nabla\mathcal{U}(\mu_1)| - \mu_2|\nabla\mathcal{U}(\mu_2)|\,\|_{\mathcal{C}^\delta(\bar\Omega)}\\ &= \|\mu_1(|\nabla\mathcal{U}(\mu_1)| - |\nabla\mathcal{U}(\mu_2)|) - (\mu_2-\mu_1)|\nabla\mathcal{U}(\mu_2)|\,\|_{\mathcal{C}^\delta(\bar\Omega)}\\ &\le \|\mu_1\|_{\mathcal{C}^\delta(\bar\Omega)}\|\,|\nabla[\mathcal{U}(\mu_1)-\mathcal{U}(\mu_2)]|\,\|_{\mathcal{C}^\delta(\bar\Omega)}\\ &\quad + K_\delta(\Omega,n,\delta)K_\mu(a,b)\|f\|_\infty\|\mu_1-\mu_2\|_{\mathcal{C}^\delta(\bar\Omega)}\\ &\le L_{\mathcal{Q}}(a,b)\|\mu_1-\mu\|_{\mathcal{C}^\delta(\bar\Omega)}.\end{aligned}$$

4.2. Proof of Theorem 2.6: Local existence. Given $\mu_0\in\mathcal{D}$ and the Lipschitz continuity of $\mathcal{Q}$ in $\mathcal{D}(a,b)$ asserted by Proposition 2.4, noting that the subspace $\mathcal{D}$ can be decomposed as given in (2.1), we may restrict our investigations on $\mathcal{D}(a,b)$. Standard arguments in the theory of ODEs in Banach spaces ensure local existence and uniqueness of the solution $\mu(t)$. In other words, there exists a sufficiently small $\tau(\mu_0)>0$ such that the fixed-point problem (2.4) admits a solution $\mu\in\mathcal{C}^0([0,\tau(\mu_0)];\mathcal{C}^\delta(\bar\Omega))$. The Lipschitz continuity of $\mathcal{Q}$ automatically ensures that $\mu\in\mathcal{C}^1([0,\tau(\mu_0)];\mathcal{C}^\delta(\bar\Omega))$. The proof of estimate (2.7) is immediate by considering that in (2.4) the term $\int_0^t e^{s-t}\mathcal{Q}(\mu(s))\,ds$ is always greater than zero.

4.3. Proof of Theorem 2.7: Lyapunov-candidate function. In this section we report the proof that $\mathcal{L}$ decreases along the trajectories. Before we compute the time derivative along the trajectories we need to prove the $\mathcal{C}^1$-regularity in time of $u(t)$. We have the following proposition (proof in subsection 4.5).

PROPOSITION 4.1. *The function $u(t)$ belongs to the space $\mathcal{C}^1([0,\tau(\mu_0)[;\mathcal{C}^{1,\delta}(\Omega))$. For each $t\in[0,\tau(\mu_0)[$ its time derivative $u'(t)$ solves the following equation:*

$$\begin{cases}\int_\Omega \mu(t)\nabla u'(t)\cdot\nabla\varphi\,dx = -\int_\Omega \mu'(t)\nabla u(t)\cdot\nabla\varphi\,dx \quad \forall\varphi\in H^1(\Omega),\\ \int_\Omega u'(t)\,dx = 0.\end{cases} \tag{4.7}$$

We can now compute the time derivative of $\mathcal{L}(\mu(t))$ and prove it is strictly negative, thus proving Theorem 2.7. In fact, we have

$$\begin{aligned}2\mathcal{L}'(t) &= \frac{d}{dt}\left(\int_\Omega \mu(t)\,dx\int_\Omega \mu(t)|\nabla u(t)|^2\,dx\right)\\ &= \int_\Omega \mu'(t)\,dx\int_\Omega \mu(t)|\nabla u(t)|^2\,dx\\ &\quad + \int_\Omega \mu(t)\,dx\int_\Omega [\mu'(t)|\nabla u(t)|^2 + 2\,\mu(t)\nabla u'(t)\cdot\nabla u(t)]\,dx.\end{aligned}$$

Substituting $\varphi = u(t)$ in (4.7) we get

$$\int_\Omega \mu(t)\nabla u'(t)\cdot\nabla u(t)\,dx = -\int_\Omega \mu'(t)|\nabla u(t)|^2\,dx.$$

Thus

$$\begin{aligned}2\mathcal{L}'(t) &= \int_\Omega \mu'(t)\,dx\int_\Omega \mu(t)|\nabla u(t)|^2\,dx - \int_\Omega \mu(t)\int_\Omega \mu'(t)|\nabla u(t)|^2\,dx\\ &= \int_\Omega \mu(t)|\nabla u(t)|\,dx\int_\Omega \mu(t)|\nabla u(t)|^2\,dx - \int_\Omega \mu(t)\,dx\int_\Omega \mu(t)|\nabla u(t)|^3\,dx.\end{aligned}$$

Rewriting the product of integrals as an integral in $\Omega \times \Omega$ of the functions

$$f(t;x,y) := \mu(t,x)|\nabla u(t,x)|\ \mu(t,y)|\nabla u(t,y)|^2 - \mu(t,x)\ \mu(t,y)|\nabla u(t,y)|^3,$$
$$g(t;x,y) := \mu(t,y)|\nabla u(t,y)|\ \mu(t,x)|\nabla u(t,x)|^2 - \mu(t,y)\ \mu(t,x)|\nabla u(t,x)|^3,$$

we obtain

$$\begin{aligned} 2\mathcal{L}'(t) &= \int_{\Omega\times\Omega} f(t;x,y)\,dx\,dy = \int_{\Omega\times\Omega} g(t;x,y)\,dx\,dy \\ &= \int_{\Omega\times\Omega} \frac{f(t;x,y)+g(t;x,y)}{2}\,dx\,dy = \int_{\Omega\times\Omega} \mu(t,x)\ \mu(t,y)\ \frac{h(t;x,y)}{2}\,dxdy, \end{aligned}$$

where

$$\begin{aligned} h(t;x,y) &= |\nabla u(t,x)|\ |\nabla u(t,y)|^2 - |\nabla u(t,y)|^3 + |\nabla u(t,x)|^2|\nabla u(t,y)| - |\nabla u(t,x)|^3 \\ &= |\nabla u(t,x)|\ |\nabla u(t,y)|\,(|\nabla u(t,x)| + |\nabla u(t,y)|) \\ &\quad - (|\nabla u(t,x)| + |\nabla u(t,y)|)\left(|\nabla u(t,x)|^2 + |\nabla u(t,y)|^2 - |\nabla u(t,x)|\ |\nabla u(t,y)|\right) \\ &= -\left(|\nabla u(t,x)| + |\nabla u(t,y)|\right)\left(|\nabla u(t,x)| - |\nabla u(t,y)|\right)^2. \end{aligned}$$

Finally, we arrive at

$$\begin{aligned} \mathcal{L}'(t) &= -\frac{1}{2}\int_{\Omega\times\Omega} \mu(t,x)\mu(t,y)\left(|\nabla u(t,x)| + |\nabla u(t,y)|\right)\left(|\nabla u(t,x)| - |\nabla u(t,y)|\right)^2\,dx\,dy \\ &\le 0. \end{aligned}$$

Remark 4.2. Note that, assuming global existence of the solution, we have that $\mathcal{L}' = 0$ only if $\mu = 0$ or $|\nabla u| = \text{const}$ for all times. In particular, this assertion provides further support to our conjecture.

4.4. Proof of Lemma 2.8: Boundedness of μ and $\mathcal{Q}$. The L^1-bound for $\mathcal{Q}(\mu(t))$ derives directly from Theorem 2.7. By the Cauchy–Schwarz inequality, we can write

$$\int_\Omega \mathcal{Q}(\mu(t))\,dx \le \left(\int_\Omega \mu(t)\,dx\ \int_\Omega \mu(t)|\nabla \mathcal{U}(\mu(t))|^2\,dx\right)^{\frac{1}{2}} = \mathcal{L}(\mu(t))^{\frac{1}{2}} \le \mathcal{L}(\mu(0))^{\frac{1}{2}}.$$

Then the L^1-bound for $\mu(t)$ is obtained by integrating both sides of (2.4) over Ω:

$$\begin{aligned} \int_\Omega \mu(t)\,dx &= e^{-t}\int_\Omega \mu_0\,dx + e^{-t}\int_0^t e^s\left(\int_\Omega \mathcal{Q}\left(\mu(s)\right)dx\right)\,ds \\ &\le e^{-t}\int_\Omega \mu_0\,dx + e^{-t}\int_0^t e^s(\mathcal{L}(\mu_0))^{\frac{1}{2}}\,ds \le \int_\Omega \mu_0\,dx + (\mathcal{L}(\mu_0))^{\frac{1}{2}}. \end{aligned}$$

4.5. Proof of Proposition 4.1: $\mathcal{C}^1$-regularity of $u(t)$. Let $t \in [0, \tau(\mu_0)[$ and choose $h > 0$ such that $t+h < \tau(\mu_0)$. The solution $\mu(t)$ of (2.3) belongs to a ball centered in μ_0 and with appropriate radius R. More detailed information on the size of this R can be drawn from the proof of Theorem 2.6. Using (2.7), it is possible to find two constants $a(\mu_0), b(\mu_0)$ such that $\mu(t) \in \mathcal{D}\left(a(\mu_0), b(\mu_0)\right)$. This allows us to write

$$K_\mu(\mu(t)) = \frac{1}{\lambda(\mu(t))}\left(\frac{\|\mu(t)\|_{\mathcal{C}^\delta(\bar\Omega)}}{\lambda(\mu(t))}\right)^{\frac{n+\delta}{2\delta}} \le \frac{1}{a(\mu_0)}\left(\frac{b(\mu_0)}{a(\mu_0)}\right)^{\frac{n+\delta}{2\delta}} \quad \forall t \in [0,\tau(\mu)[$$

which shows that both the potential and flux operators are bounded and Lipschitz-continuous in $\mathcal{D}\left(a(\mu_0), b(\mu_0)\right)$.

Heuristically, the proof is based on the observation that, assuming existence of both μ' and u', we can take the derivative in time of (2.2a) and use the fact that the source function is independent of time, thus obtaining (4.7). We first note that $u(t) = \mathcal{U}(\mu(t))$ is Lipschitz continuous in time, since $\mathcal{U}$ is locally Lipschitz continuous and $\mu \in \mathcal{C}^1\left([0, \tau(\mu_0)[\,; \mathcal{C}^\delta(\bar{\Omega})\right)$. Next at each time $t \in [0, \tau(\mu_0)[$, we define $w(t)$, that heuristically should be $u'(t)$, as the unique solution of

$$\begin{aligned} &\int_\Omega \mu(t)\nabla w(t)\cdot\nabla\varphi\,dx = -\int_\Omega \mu'(t)\nabla u(t)\cdot\nabla\varphi\,dx \quad \forall\varphi\in H^1(\Omega),\\ &\int_\Omega w(t)\,dx = 0. \end{aligned} \tag{4.8}$$

It is easy to verify that $w(t) \in \mathcal{C}^{1,\delta}(\bar{\Omega})$. Hence $\forall\varphi \in H^1(\Omega)$ we can write

$$\int_\Omega \mu(t)\nabla u(t)\cdot\nabla\varphi\,dx = \int_\Omega f\varphi\,dx = \int_\Omega \mu(t{+}h)\nabla u(t{+}h)\cdot\nabla\varphi\,dx.$$

Changing sign and adding on both sides $\int_\Omega \mu(t)\nabla u(t{+}h)\cdot\nabla\varphi\,dx$, yields

$$\int_\Omega \mu(t)\nabla[u(t{+}h)-u(t)]\cdot\nabla\varphi\,dx = -\int_\Omega [\mu(t{+}h)-\mu(t)]\nabla u(t{+}h)\cdot\nabla\varphi\,dx. \tag{4.9}$$

Now we multiply (4.8) by $-h$ and sum (4.8) and (4.9) to obtain

$$\begin{aligned} &\int_\Omega \mu(t)\nabla[u(t{+}h)-u(t)-hw(t)]\cdot\nabla\varphi\,dx\\ &\quad= -\int_\Omega [\mu(t{+}h)-\mu(t)]\nabla u(t{+}h)\cdot\nabla\varphi\,dx + h\int_\Omega \mu'(t)\nabla u(t)\cdot\nabla\varphi\,dx\\ &\quad= -\int_\Omega [G_1(t,h) + h\,G_2(t,h)]\cdot\nabla\varphi\,dx \end{aligned}$$

with

$$G_1(t,h) = [\mu(t{+}h)-\mu(t)-h\mu'(t)]\,\nabla u(t{+}h), \quad G_2(t,h) = \mu'(t)\,[\nabla u(t{+}h)-\nabla u(t)]\,.$$

Since $\mu \in \mathcal{C}^1(0,\tau;\mathcal{C}^\delta(\bar{\Omega}))$, we can estimate the above functions G_1 and G_2 as

$$\begin{aligned} \|G_1(t,h)\|_{\mathcal{C}^\delta(\bar{\Omega})} &\le \|\mu(t{+}h)-\mu(t)-h\mu'(t)\|_{\mathcal{C}^\delta(\bar{\Omega})}\|\nabla u(t{+}h)\|_{\mathcal{C}^\delta(\bar{\Omega})}\\ &\le K_\delta(n,\Omega,\delta)K_\mu(\mu(t))\|f\|_{L^\infty(\Omega)}\cdot o(h)\\ &\le K_\delta(n,\Omega,\delta)K(\mu_0)\|f\|_{L^\infty(\Omega)}\cdot o(h) \end{aligned}$$

and, since the potential operator is Lipschitz continuous, we also have

$$\begin{aligned} \|G_2(t,h)\|_{\mathcal{C}^\delta(\bar{\Omega})} &= \|\mu'(t)\,[\nabla u(t{+}h)-\nabla u(t)]\,\|_{\mathcal{C}^\delta(\bar{\Omega})}\\ &\le \|\mu'(t)\|_{\mathcal{C}^\delta(\bar{\Omega})}\|\nabla u(t{+}h)-\nabla u(t)\|_{\mathcal{C}^\delta(\bar{\Omega})}\\ &\le L(\mu_0)h, \end{aligned}$$

where $L(\mu_0)$ is a function of f, K_δ. Thus we can write

$$\|G_1 + hG_2\|_{\mathcal{C}^\delta(\bar{\Omega})} \le \|G_1\|_{\mathcal{C}^\delta(\bar{\Omega})} + \|G_2\|_{\mathcal{C}^\delta(\bar{\Omega})} = o(h)$$

and, for Lemma 2.5 using $F = -(G_1 + hG_2)$, we obtain

$$\lim_{h\to 0} \frac{\|\nabla[u(t+h) - u(t) - hw(t)]\|_{\mathcal{C}^\delta(\bar\Omega)}}{h} = 0$$

that shows that $u' \in \mathcal{C}^1(0,\tau;\mathcal{C}^\delta(\bar\Omega))$ with $u' = w$.

4.6. Proof of Lemma 2.5: Elliptic regularity. Lemma 2.5 is analogous to Theorem 5.19 of [16] simplified to a scalar elliptic equation but extended to explicitly determine the dependence of the inequality constants upon μ. We will denote with C or c generic constants that may depend upon n, Ω, and the Hölder continuity exponent δ but are always independent of μ. We will use the following result adapted from Proposition 5.8 in [16].

LEMMA 4.3 (elliptic decay). *Let $v \in H^1(\Omega)$ be any solution of*

$$\int_\Omega \nabla v \nabla \varphi \, dx = 0 \quad \forall \varphi \in H^1_0(\Omega); \tag{4.10}$$

then there exists a constant $c(n)$ such that

$$\int_{B(x_0,\rho)} |\nabla v|^2 \, dx \le c(n) \left(\frac{\rho}{R}\right)^n \int_{B(x_0,R)} |\nabla v|^2 \, dx, \tag{4.11}$$

$$\int_{B(x_0,\rho)} |\nabla v - (\nabla v)_{x_0,\rho}|^2 \, dx \le c(n) \left(\frac{\rho}{R}\right)^{n+2} \int_{B(x_0,R)} |\nabla v - (\nabla v)_{x_0,R}|^2 \, dx \tag{4.12}$$

for arbitrary balls $B(x_0,\rho) \Subset B(x_0,R) \Subset \Omega$.

Our case follows from the observation that the derivatives of v satisfy the weak form of Laplace equation (see also [3, page 61]). Note that the constant $c(n)$ depends only on the problem dimension n as we are considering the Laplace equation.

We also use the following result from Lemma 5.13 in [16] and Lemma 9.2 in [2].

LEMMA 4.4 (iteration lemma). *Let $\phi : \mathbb{R}^+ \mapsto \mathbb{R}^+$ be a nonnegative and nonincreasing function satisfying*

$$\phi(\rho) \le A \left[\left(\frac{\rho}{R}\right)^\alpha + \epsilon\right] \phi(R) + B\, R^\beta \tag{4.13}$$

for some $A, \alpha, \beta > 0$, with $\alpha > \beta$, and for all $0 < \rho \le R \le R_0$, where $R_0 > 0$ is given.

Then there exist constants $\epsilon_0 = \epsilon_0(A,\alpha,\beta)$ and $C = C(A,\alpha,\beta)$ such that

$$\text{if} \quad \epsilon \le \epsilon_0 = \left(\frac{1}{2A}\right)^{\frac{2\alpha}{\alpha-\beta}} \quad \text{then} \quad \phi(\rho) \le C \left[\frac{\phi(R)}{R^\beta} + B\right] \rho^\beta. \tag{4.14}$$

The proof of Lemma 2.5 uses a classical bootstrap technique introduced by [17, 11] and used more recently by [12] to show the regularity of local minimizers of double phase variational integrals. The technique can be described by the following steps. First we consider a compact set $K \Subset \Omega$ and prove that $u \in L^{2,\nu}(K)$ for a suitable regularity exponent ν with $0 < \nu < n$. Then, $u \in \mathcal{L}^{2,n+2\delta}(K)$, where $L^{2,\nu}(K)$ and $\mathcal{L}^{2,n+2\delta}(K)$ are the Morrey and Campanato spaces, respectively. The results are extended to the entire domain by assuming enough regularity of $\partial\Omega$. This latter step is not reported in the following proof for brevity. Finally, the equivalence between the Campanato spaces $\mathcal{L}^{2,n+2\delta}(\Omega)$ and $\mathcal{C}^\delta(\bar\Omega)$ is used to prove estimate (2.5) and to

derive the expression of the constant K_μ given in (2.6). We recall that the norm of a function $u : \Omega \to \mathbb{R}^m$ (in our case we have either $m = 1$ or $m = n$) belonging to a Morrey space is given by

$$\|u\|_{L^{2,\gamma}(\Omega)} = \Big(\sup_{\substack{x_0 \in \Omega \\ \rho > 0}} \rho^{-\gamma} \int_{\Omega(x_0,\rho)} |u|^2 \, dx \Big)^{\frac{1}{2}},$$

where $\Omega(x_0, \rho) = \Omega \cap B(x_0, \rho)$ and $0 \le \gamma < n$. For $0 \le \gamma < n + 2$, the norm of u belonging to a Campanato space is given by

$$\|u\|_{\mathcal{L}^{2,\gamma}(\Omega)} = \|u\|_{L^2(\Omega)} + \Big(\sup_{\substack{x_0 \in \Omega \\ \rho > 0}} \rho^{-\gamma} \int_{\Omega(x_0,\rho)} |u - (u)_{x_0,\rho}|^2 \, dx \Big)^{\frac{1}{2}},$$

where $(u)_{x_0,\rho} = \int_{\Omega(x_0,\rho)} u \, dx / |\Omega(x_0, \rho)|$ is the average integral.

Proof. The first step of the bootstrap proceeds as follows. Consider $x_0 \in K$ and the ball $B_R := B(x_0, R) \Subset \Omega$. In this ball we use Korn's technique (freezing the coefficients) to decompose the solution as $u = v + w$, where $v \in H^1(B_R)$ satisfies the equations

$$\int_{B_R} \mu(x_0) \nabla v \nabla \varphi \, dx = 0 \quad \forall \varphi \in H^1_0(B_R) \tag{4.15}$$

with $v = u$ in ∂B_R and the second equation is to be interpreted in the sense that $v - u \in H^1_0(B_R)$. The second function $w \in H^1_0(B_R)$ satisfies the equation

$$\begin{aligned} &\int_{B_R} \mu(x_0) \nabla w \nabla \varphi \, dx \\ &\quad = \int_{B_R} \Big[F_0 \varphi + F \cdot \nabla \varphi - (\mu(x) - \mu(x_0)) \, \nabla u \cdot \nabla \varphi \Big] \, dx \qquad \forall \varphi \in H^1_0(B_R) \end{aligned} \tag{4.16}$$

with $w = 0$ in ∂B_R. Since $\mu(x_0)$ in (4.15) is a strictly positive and bounded scalar number it can be eliminated from the equation, hence w simply solves the weak form of the Laplace equation:

$$\int_{B_R} \nabla v \nabla \varphi \, dx = 0 \qquad \forall \varphi \in H^1_0(\Omega) \tag{4.17}$$

with $v = u$ in $\partial\Omega$. Thus we can use Lemma 4.3 to obtain

$$\int_{B_\rho} |\nabla v|^2 \, dx \le c(n) \Big(\frac{\rho}{R} \Big)^n \int_{B_R} |\nabla v|^2 \, dx. \tag{4.18}$$

Recall that at this point our goal is to estimate the Morrey norm $\|\nabla u\|_{L^{2,\nu}(K)}$ with $\nu < n$. We use the above decomposition of u to estimate $\phi(\rho) := \int_{B_\rho} |\nabla u|^2 \, dx$,

$0 < \rho \le R$. Thus we can write:

$$\begin{aligned}\int_{B_\rho} |\nabla u|^2\,dx &= \int_{B_\rho} |\nabla v + \nabla w|^2\,dx \le 2\int_{B_\rho} |\nabla v|^2\,dx + 2\int_{B_\rho} |\nabla w|^2\,dx\\ &\le c(n)\left(\frac{\rho}{R}\right)^n \int_{B_R} |\nabla v|^2\,dx + 2\int_{B_\rho} |\nabla w|^2\,dx\\ &= c(n)\left(\frac{\rho}{R}\right)^n \int_{B_R} |\nabla u - \nabla w|^2\,dx + 2\int_{B_\rho} |\nabla w|^2\,dx\\ &\le c(n)\left(\frac{\rho}{R}\right)^n \int_{B_R} |\nabla u|^2\,dx + c(n)\left(\frac{\rho}{R}\right)^n \int_{B_\rho} |\nabla w|^2\,dx\\ &\quad + 2\int_{B_\rho} |\nabla w|^2\,dx\\ &\le c(n)\left(\frac{\rho}{R}\right)^n \int_{B_R} |\nabla u|^2\,dx + c(n)\int_{B_R} |\nabla w|^2\,dx.\end{aligned}$$

Note that, somewhat improperly, we always use the symbol $c(n)$ to indicate a constant depending on n only and that it may assume a different meaning even within the same equation. To estimate $\int_{B_R} |\nabla w|^2\,dx$ we use $\varphi = w$ in (4.16) to get

$$\begin{aligned}\lambda(\mu)\int_{B_R} |\nabla w|^2\,dx &\le \int_{B_R} \mu(x_0)|\nabla w|^2\,dx\\ &= \int_{B_R} \left[F_0 w + F\cdot\nabla w - (\mu(x) - \mu(x_0))\,\nabla u \nabla w\right]\,dx.\end{aligned} \tag{4.19}$$

Using the Hölder continuity of μ, and the Poincaré and Cauchy–Schwarz inequalities, we can bound the right-hand side of the previous equation to obtain

$$\int_{B(x_0,R)} F_0 w\,dx \le \|F_0\|_{L^2(B(x_0,R))}\, c(n)\, \|\nabla w\|_{L^2(B(x_0,R))},$$

$$\int_{B(x_0,R)} F\cdot\nabla w\,dx \le \|F\|_{L^2(B(x_0,R))}\, \|\nabla w\|_{L^2(B(x_0,R))},$$

$$\int_{B(x_0,R)} (\mu(x) - \mu(x_0))\,\nabla u\nabla w\,dx \le R^\delta \|\mu\|_{\mathcal{C}^\delta(\bar\Omega)} \|\nabla u\|_{L^2(B(x_0,R))}\, \|\nabla w\|_{L^2(B(x_0,R))}.$$

In the end, using the Minkowski inequality to remove the double products, we can write

$$\begin{aligned}\int_{B_R} |\nabla w|^2\,dx \le 2\frac{1}{(\lambda(\mu))^2}\Big[&(c(n))^2\|F_0\|^2_{L^2(B_R)}\\ &+ \|F\|^2_{L^2(B_R)} + R^{2\delta}\|\mu\|^2_{\mathcal{C}^\delta(\bar\Omega)}\|\nabla u\|^2_{L^2(B_R)}\Big].\end{aligned} \tag{4.20}$$

Since $F_0 \in L^\infty(\Omega)$, implying that $F_0 \in L^{2,\nu}(\Omega)$ and $\|F_0\|^2_{L^{2,\nu}(\Omega)} \le c(n)\|F_0\|^2_{L^\infty(\Omega)}$ for

$0 \le \nu < n$, we obtain

$$\|F_0\|^2_{L^2(B_R)} \le c(n)\|F_0\|^2_{L^\infty(B_R)} R^\nu \le c(n)\|F_0\|^2_{L^\infty(\Omega)} R^\nu. \tag{4.21}$$

Since $F \in \mathcal{C}^\delta(\bar\Omega)$ implies that (each component of) $F \in \mathcal{L}^{2,\gamma}(\Omega)$ for all $0 \le \gamma \le n+2\delta$, noting that we require $0 \le \nu < n$ and in this case $L^{2,\nu}(\Omega) \equiv \mathcal{L}^{2,\nu}(\Omega)$, we obtain

$$\|F\|^2_{L^2(B_R)} \le \|F\|^2_{\mathcal{L}^{2,\gamma}(B_R)} R^\gamma \le c(n)\|F\|^2_{\mathcal{C}^\delta(\bar\Omega)} R^\gamma. \tag{4.22}$$

Taking $\nu < n$ in (4.21) and $\gamma = \nu$ in (4.22) we get

$$\begin{aligned}\int_{B_\rho} |\nabla u|^2\,dx \le c(n)\left[\left(\frac{\rho}{R}\right)^n + R^{2\delta}\left(\frac{\|\mu\|_{\mathcal{C}^\delta(\bar\Omega)}}{\lambda(\mu)}\right)^2\right]\int_{B_R} |\nabla u|^2\,dx \\ + c(n)\left(\frac{\|F_0\|^2_{L^\infty(\Omega)} + \|F\|^2_{\mathcal{C}^\delta(\bar\Omega)}}{(\lambda(\mu))^2}\right) R^\nu.\end{aligned} \tag{4.23}$$

Now we rewrite inequality (4.23) in the form of the hypotheses of Lemma 4.4, i.e.,

$$\phi(\rho) := \int_{B_\rho} |\nabla u|^2\,dx, \qquad \alpha = n,\ \beta = \nu,$$

$$\epsilon = R^{2\delta}\left(\frac{\|\mu\|_{\mathcal{C}^\delta(\bar\Omega)}}{\lambda(\mu)}\right)^2,\ A = c(n),\ B = c(n)\left(\frac{\|F_0\|^2_{L^\infty(\Omega)} + \|F\|^2_{\mathcal{C}^\delta(\bar\Omega)}}{(\lambda(\mu))^2}\right)$$

for $\rho \le R$. Considering R such that

$$R^{2\delta}\left(\frac{\|\mu\|_{\mathcal{C}^\delta(\bar\Omega)}}{\lambda(\mu)}\right)^2 \le \left(\frac{1}{2A}\right)^{\frac{2n}{n-\nu}} = A_0,$$

we have that

$$R \le R_0 = A_0^{\frac{1}{2\delta}}\left(\frac{\lambda(\mu)}{\|\mu\|_{\mathcal{C}^\delta(\bar\Omega)}}\right)^{\frac{1}{\delta}}, \tag{4.24}$$

We can now apply Lemma 4.4 to arrive at the following estimate valid for $0 < \rho \le R \le R_0$:

$$\int_{B_\rho} |\nabla u|^2\,dx \le C(A,n,\nu)\rho^\nu\left(\frac{\int_{B_R}|\nabla u|^2\,dx}{R^\nu} + B\right). \tag{4.25}$$

Incorporating all the constants into one single constant $C(n,\nu)$ we obtain

$$\int_{B_\rho} |\nabla u|^2\,dx \le C(n,\nu)\rho^\nu\left(\frac{\int_{B_R}|\nabla u|^2\,dx}{R^\nu} + \frac{\|F_0\|^2_{L^\infty(\Omega)} + \|F\|^2_{\mathcal{C}^\delta(\bar\Omega)}}{(\lambda(\mu))^2}\right). \tag{4.26}$$

The previous estimate is valid for every $B_R \Subset \Omega$. Varying $x_0 \in K$ and using the continuity inequality in the Lax–Milgram lemma we obtain the desired estimate of

this first step of the bootstrap procedure, i.e.,

$$\begin{aligned}\|\nabla u\|^2_{L^{2,\nu}(K)} &\le C(n,\nu)\left(\frac{\int_{B_{R_0}}|\nabla u|^2\,dx}{R_0^\nu}+\frac{\|F_0\|^2_{L^\infty(\Omega)}+\|F\|^2_{\mathcal{C}^\delta(\bar\Omega)}}{(\lambda(\mu))^2}\right)\\ &\le C(n,\nu)\left(\frac{C(\Omega)\|F_0\|^2_{L^\infty(\Omega)}+\|F\|^2_{\mathcal{C}^\delta(\bar\Omega)}}{(\lambda(\mu))^2}\frac{1}{R_0^\mu}+\frac{\|F_0\|^2_{L^\infty(\Omega)}+\|F\|^2_{\mathcal{C}^\delta(\bar\Omega)}}{(\lambda(\mu))^2}\right)\\ &\le C(n,\nu)C(\Omega)\frac{\|F_0\|^2_{L^\infty(\Omega)}+\|F\|^2_{\mathcal{C}^\delta(\bar\Omega)}}{(\lambda(\mu))^2}\left(\frac{\|\mu\|_{\mathcal{C}^\delta(\bar\Omega)}}{\lambda(\mu)}\right)^{\frac{\nu}{\delta}},\end{aligned}\tag{4.27}$$

where $C(n,\nu)$ is bounded for all $\nu<n$.

The second step of the bootstrap procedure starts by noting that (4.16) can be rewritten using $R=R_0$ as defined above:

$$\begin{aligned}&\int_{B_R}\mu(x_0)\nabla w\nabla\varphi\,dx\\ &\quad=\int_{B_R}\Big[F_0\varphi+(F-(F)_R)\cdot\nabla\varphi-(\mu(x)-\mu(x_0))\,\nabla u\cdot\nabla\varphi\Big]\,dx\quad\forall\varphi\in H^1_0(B_R),\\ &w=0\text{ in }\ \partial B_R.\end{aligned}\tag{4.28}$$

We continue by again using the decomposition $u=v+w$ and Lemma 4.3 to obtain

$$\begin{aligned}\int_{B_\rho}|\nabla u-(\nabla u)_\rho|^2\,dx&=\int_{B_\rho}|\nabla v+(\nabla v)_\rho+\nabla w+(\nabla w)_\rho|^2\,dx\\ &\le c(n)\left(\frac{\rho}{R}\right)^{n+2}\int_{B_R}|\nabla v-(\nabla v)_R|^2\,dx+2\int_{B_\rho}|\nabla w-(\nabla w)_\rho|^2\,dx\\ &\le c(n)\left(\frac{\rho}{R}\right)^{n+2}\int_{B_R}|\nabla u-(\nabla u)_R|^2\,dx+c(n)\int_{B_R}|\nabla w|^2\,dx,\end{aligned}$$

where the last inequality arises from the minimality of the mean. We follow the same developments as before, but now we explicitly include the factor R in the constant of the Poincaré inequality to obtain

$$\begin{aligned}\int_{B_\rho}|\nabla u-(\nabla u)_\rho|^2\,dx&\le c(n)\left(\frac{\rho}{R}\right)^{n+2}\int_{B_R}|\nabla u-(\nabla u)_R|^2\,dx\\ &+2c(n)\frac{R^2\|F_0\|^2_{L^2(B_R)}+\|F-(F)_R\|^2_{L^2(B_R)}+R^{2\delta}\|\mu\|^2_{\mathcal{C}^\delta(\bar\Omega)}\|\nabla u\|^2_{L^2(B_R)}}{(\lambda(\mu))^2}.\end{aligned}\tag{4.29}$$

Since $\nabla u\in L^{2,\nu}(K)$ for $0<\nu<n$ we can take $\nu=n-\delta$ in (4.27) to get

$$\|\nabla u\|^2_{L^2(B_R)}=\frac{\int_{B_R}|\nabla u|^2\,dx}{R^{n-\delta}}R^{n-\delta}\le\|\nabla u\|_{L^{2,n-\delta}}R^{n-\delta}.$$

Using $\nu=n-2+\delta$ in (4.21) we obtain $\|F_0\|^2_{L^2(B_R)}\le c(n)\|F_0\|^2_{L^\infty(\Omega)}R^{n-2+\delta}$, while using $\gamma=n+\delta$ in (4.22) we have $\|F-(F)_R\|^2_{L^2(B_R)}\le\|F\|^2_{\mathcal{C}^\delta(\bar\Omega)}R^{n+\delta}$. Substitution

of these inequalities into (4.29) yields

$$\begin{aligned}
&\int_{B_\rho} |\nabla u - (\nabla u)_\rho|^2\,dx \le c(n)\left(\frac{\rho}{R}\right)^{n+2}\int_{B_R}|\nabla u-(\nabla u)_R|^2\,dx\\
&\quad + c(n)\frac{\|F_0\|^2_{L^\infty(\Omega)}+\|F\|^2_{\mathcal{C}^\delta(\bar\Omega)}}{(\lambda(\mu))^2}R^{n+\delta}\\
&\quad + R^{2\delta}\frac{\|\mu\|^2_{\mathcal{C}^\delta(\bar\Omega)}}{(\lambda(\mu))^2}C(n,n-\delta)C(\Omega)\frac{\|F_0\|^2_{L^\infty(\Omega)}+\|F\|^2_{\mathcal{C}^\delta(\bar\Omega)}}{(\lambda(\mu))^2}\left(\left(\frac{\|\mu\|_{\mathcal{C}^\delta(\bar\Omega)}}{\lambda(\mu)}\right)^{\frac{n-\delta}{\delta}}\right)R^{n-\delta}\\
&\le c(n)\left(\frac{\rho}{R}\right)^{n+2}\int_{B_R}|\nabla u-(\nabla u)_R|^2\,dx\\
&\quad + C(n,\Omega,\delta)\frac{\|F_0\|^2_{L^\infty(\Omega)}+\|F\|^2_{\mathcal{C}^\delta(\bar\Omega)}}{(\lambda(\mu))^2}\left(1+\frac{\|\mu\|^2_{\mathcal{C}^\delta(\bar\Omega)}}{(\lambda(\mu))^2}\left(\frac{\|\mu\|_{\mathcal{C}^\delta(\bar\Omega)}}{\lambda(\mu)}\right)^{\frac{n-\delta}{\delta}}\right)R^{n+\delta}\\
&\le c(n)\left(\frac{\rho}{R}\right)^{n+2}\int_{B_R}|\nabla u-(\nabla u)_R|^2\,dx\\
&\quad + C(n,\Omega,\delta)\frac{\|F_0\|^2_{L^\infty(\Omega)}+\|F\|^2_{\mathcal{C}^\delta(\bar\Omega)}}{(\lambda(\mu))^2}\left(\frac{\|\mu\|_{\mathcal{C}^\delta(\bar\Omega)}}{\lambda(\mu)}\right)^{\frac{n+\delta}{\delta}}R^{n+\delta}.
\end{aligned}$$

Application of Lemma 4.4 with $\phi(\rho) := \int_{B_\rho}|\nabla u-(\nabla u)_\rho|^2\,dx$ yields, for $0<\rho\le R\le R_0$,

$$\begin{aligned}
&\int_{B_\rho}|\nabla u-(\nabla u)_\rho|^2\,dx \le \rho^{n+\delta}C(n,\Omega,\delta)\\
&\quad\cdot\left[\frac{\int_{B_R}|\nabla u-(\nabla u)_R|^2\,dx}{R^{n+\delta}}+\left(\frac{\|F_0\|^2_{L^\infty(\Omega)}+\|F\|^2_{\mathcal{C}^\delta(\bar\Omega)}}{\lambda(\mu)^2}\right)\left(\frac{\|\mu\|_{\mathcal{C}^\delta(\bar\Omega)}}{\lambda(\mu)}\right)^{\frac{n}{\delta}+1}\right]
\end{aligned}$$

from which, using again the minimality of the mean and the estimate of R_0 given in (4.24), we can evaluate

$$\begin{aligned}
&\frac{\int_{B_\rho}|\nabla u-(\nabla u)_\rho|^2\,dx}{\rho^{n+\delta}} \le C(n,\delta,\Omega)\\
&\qquad\cdot\left[\frac{\int_{B_{R_0}}|\nabla u-(\nabla u)_{R_0}|^2\,dx}{R_0^{n+\delta}}+\left(\frac{\|F_0\|^2_{L^\infty(\Omega)}+\|F\|^2_{\mathcal{C}^\delta(\bar\Omega)}}{\lambda(\mu)^2}\right)\left(\frac{\|\mu\|_{\mathcal{C}^\delta(\bar\Omega)}}{\lambda(\mu)}\right)^{\frac{n}{\delta}+1}\right]\\
&\quad\le C(n,\delta,\Omega)\left(\int_{B_{R_0}}|\nabla u-(\nabla u)_{R_0}|^2\,dx+\frac{\|F_0\|^2_{L^\infty(\Omega)}+\|F\|^2_{\mathcal{C}^\delta(\bar\Omega)}}{\lambda(\mu)^2}\right)\left(\frac{\|\mu\|_{\mathcal{C}^\delta(\bar\Omega)}}{\lambda(\mu)}\right)^{\frac{n}{\delta}+1}\\
&\quad\le C(n,\delta,\Omega)\left(\int_\Omega|\nabla u|^2\,dx+\frac{\|F_0\|^2_{L^\infty(\Omega)}+\|F\|^2_{\mathcal{C}^\delta(\bar\Omega)}}{\lambda(\mu)^2}\right)\left(\frac{\|\mu\|_{\mathcal{C}^\delta(\bar\Omega)}}{\lambda(\mu)}\right)^{\frac{n}{\delta}+1}\\
&\quad\le C(n,\delta,\Omega)\left(\frac{\|F_0\|^2_{L^\infty(\Omega)}+\|F\|^2_{\mathcal{C}^\delta(\bar\Omega)}}{\lambda(\mu)^2}\right)\left(\frac{\|\mu\|_{\mathcal{C}^\delta(\bar\Omega)}}{\lambda(\mu)}\right)^{\frac{n}{\delta}+1},
\end{aligned}$$

Hence $\nabla u\in\mathcal{L}^{2,n+\delta}(K)$ and we can write

$$\|\nabla u\|^2_{\mathcal{L}^{2,n+\delta}(K)} \le C(n,\delta,\Omega)\left(\frac{\|F_0\|^2_{L^\infty(\Omega)}+\|F\|^2_{\mathcal{C}^\delta(\bar\Omega)}}{\lambda(\mu)^2}\right)\left(\frac{\|\mu\|_{\mathcal{C}^\delta(\bar\Omega)}}{\lambda(\mu)}\right)^{\frac{n}{\delta}+1}. \tag{4.30}$$

The bootstrap procedure is restarted from Proof 1 using $\nu = n - 2 + 2\delta$ in (4.21) and $\gamma = n + 2\delta$ in (4.22), and estimate (4.30) in (4.29) so that a term $R^{n+2\delta}$ can be factored. Thus we can write

$$\begin{aligned}\int_{B_\rho} |\nabla u - (\nabla u)_\rho|^2\,dx &\le c(n)\left(\frac{\rho}{R}\right)^{n+2}\int_{B_R}|\nabla u-(\nabla u)_R|^2\,dx\\ &+ c(n)\frac{\|F_0\|^2_{L^\infty(\Omega)}+\|F\|_{\mathcal{C}^\delta(\bar\Omega)}}{(\lambda(\mu))^2}R^{n+2\delta}\\ &+ C(n,\delta,\Omega)\frac{\|F_0\|^2_{L^\infty(\Omega)}+\|F\|^2_{\mathcal{C}^\delta(\bar\Omega)}}{\lambda(\mu)^2}\left(\frac{\|\mu\|_{\mathcal{C}^\delta(\bar\Omega)}}{\lambda(\mu)}\right)^{\frac{n}{\delta}+1}R^{n+2\delta}\end{aligned}$$

and, finally, applying once again Lemma 4.4, we have the final result

$$\|\nabla u\|^2_{\mathcal{L}^{2,n+2\delta}(K)} \le C(n,\delta,\Omega)\frac{\|F_0\|^2_{L^\infty(\Omega)}+\|F\|^2_{\mathcal{C}^\delta(\bar\Omega)}}{\lambda(\mu)^2}\left(\frac{\|\mu\|_{\mathcal{C}^\delta(\bar\Omega)}}{\lambda(\mu)}\right)^{\frac{n}{\delta}+1}. \tag{4.31}$$

Extension of the previous estimate to the entire domain Ω can be obtained following the same bootstrap procedure starting from the analogue of the elliptic decay Lemma 4.3 on hemispheres (similarly to what is proposed in [16, Theorem 5.21]). Such a process introduces a dependence on the regularity of the boundary $\partial\Omega$ in the constant $C(n,\delta,\Omega)$ in (4.31), but we do not explicitly write such a dependence. By the equivalence between $\mathcal{L}^{2,n+2\delta}(\Omega)$ and $\mathcal{C}^\delta(\bar\Omega)$ we get

$$\|\nabla u\|_{\mathcal{C}^\delta(\bar\Omega)} \le C(n,\delta,\Omega)\frac{\|F_0\|_{L^\infty(\Omega)}+\|F\|_{\mathcal{C}^\delta(\bar\Omega)}}{\lambda(\mu)}\left(\frac{\|\mu\|_{\mathcal{C}^\delta(\bar\Omega)}}{\lambda(\mu)}\right)^{\frac{n+\delta}{2\delta}}$$

which proves (2.5) and (2.6). From this, using Theorem 1.40 of [21], we directly obtain that $u \in \mathcal{C}^{1,\delta}(\bar\Omega)$. ∎

Acknowledgment. The authors are profoundly indebted to Giuseppe De Marco for his continuous stimulation and his important contributions during the development of this work.

REFERENCES

[1] A. Adamatzky, *Physarum Machines: Computers from Slime Mould*, World Scientific, Singapore, 2010.
[2] L. Ambrosio, *Lecture notes on optimal transport problems*, in Mathematial Aspects of Evolving Interfaces, Lecture Notes in Math. 1812, Springer, Berlin, 2003, pp. 1–52.
[3] L. Ambrosio, A. Carlotto, and A. Massaccesi, *Lecture Notes on Partial Differential Equations*, http://cvgmt.sns.it/paper/1280/ (2010).
[4] J. W. Barrett and L. Prigozhin, *A mixed formulation of the Monge-Kantorovich equations*, Math. Model. Numer. Anal., 41 (2007), pp. 1041–1060.
[5] P. Bochev and R. B. Lehoucq, *On the Finite Element Solution of the Pure Neumann Problem*, SIAM Rev., 47 (2005), pp. 50–66.
[6] V. Bonifaci, K. Mehlhorn, and G. Varma, *Physarum can compute shortest paths*, J. Theoret. Biol., 309 (2012), pp. 121–133.
[7] V. Bonifaci, K. Mehlhorn, and G. Varma, *Physarum can compute shortest paths: A short proof*, in Proceedings of the Twenty-Third Annual ACM-SIAM Symposium on Discrete Algorithms, SODA 2012, Kyoto, Japan, 2012, SIAM, Philadelphia, 2012, pp. 233–240.
[8] G. Bouchitté, G. Buttazzo, and P. Seppecher, *Shape optimization solutions via Monge-Kantorovich equation*, C. R. Acad. Sci. Paris Ser. I Math, 324 (1997), pp. 1185–1191.
[9] F. Brezzi and M. Fortin, *Mixed and Hybrid Finite Element Methods*, Springer, Berlin, 1991.
[10] G. Buttazzo and E. Stepanov, *On regularity of transport density in the Monge–Kantorovich problem.*, SIAM J. Control Optim., 42 (2003), pp. 1044–1055.

[11] S. Campanato, *Equazioni ellittiche del ii^o ordine e spazi* $\mathfrak{L}^{(2,\lambda)}$, Ann. Mat. Pura Appl. (4), 69 (1965), pp. 321–381.
[12] M. Colombo and G. Mingione, *Bounded minimisers of double phase variational integrals*, Arch. Ration. Mech. Anal., 218 (2015), pp. 219–273.
[13] L. De Pascale and A. Pratelli, *Sharp summability for Monge transport density via interpolation*, ESAIM Control Optim, Calc. Var., 10 (2004), pp. 549–552.
[14] L. C. Evans and W. Gangbo, *Differential Equations Methods for the Monge-Kantorovich Mass Transfer Problem*, Mem. Amer. Math. Soc., 653, AMS, Providence, RI, 1999.
[15] M. Feldman and R. J. McCann, *Uniqueness and transport density in Monge's mass transportation problem*, Calc. Var. Partial Differential Equations, 15 (2002), pp. 81–113.
[16] M. Giaquinta and L. Martinazzi, *An Introduction to the Regularity Theory for Elliptic Systems, Harmonic Maps and Minimal Graphs*, Edizione della Normale, Pisa, 2012.
[17] C. B. Morrey Jr, *Second-order elliptic systems of differential equations*, in Contributions to the Theory of Partial Differential Equations, Princeton University Press, Princeton, NJ, 1954, pp. 101–159.
[18] T. Nakagaki, H. Yamada, and A. Toth, *Maze-solving by an amoeboid organism*, Nature, 407 (2000), 470.
[19] A. Tero, R. Kobayashi, and T. Nakagaki, *A mathematical model for adaptive transport network in path finding by true slime mold*, J. Theoret. Biol., 244 (2007), pp. 553–564.
[20] A. Tero, S. Takagi, T. Saigusa, K. Ito, D. P. Bebber, M. D. Fricker, K. Yumiki, R. Kobayashi, and T. Nakagaki, *Rules for biologically inspired adaptive network design.*, Science, 327 (2010), pp. 439–442.
[21] G. Troianiello, *Elliptic Differential Equations and Obstacle Problems*, Univ. Ser. Math., Plenum, New York, 1987.